Regulation of Microtubule-dependent Recycling at the *Trans*-Golgi Network by Rab6A and Rab6A' □

Joanne Young, Tobias Stauber, Elaine del Nery, Isabelle Vernos, Rainer Pepperkok,*† and Tommy Nilsson*†‡

Cell Biology and Biophysics Programme, European Molecular Biology Laboratory, D-69117 Heidelberg, Germany

The small GTPase rab6A but not the isoform rab6A' has previously been identified as a regulator of the COPI-independent recycling route that carries Golgi-resident proteins and certain toxins from the Golgi to the endoplasmic reticulum (ER). The isoform rab6A' has been implicated in Golgi-to-endosomal recycling. Because rab6A but not A', binds rabkinesin6, this motor protein is proposed to mediate COPI-independent recycling. We show here that both rab6A and rab6A' GTP-restricted mutants promote, with similar efficiency, a microtubule-dependent recycling of Golgi resident glycosylation enzymes upon overexpression. Moreover, we used small interfering RNA mediated down-regulation of rab6A and A' expression and found that reduced levels of rab6 perturbs organization of the Golgi apparatus and delays Golgi-to-ER recycling. Rab6-directed Golgi-to-ER recycling seems to require functional dynactin, as overexpression of p50/dynamitin, or a C-terminal fragment of Bicaudal-D, both known to interact with dynactin inhibit recycling. We further present evidence that rab6-mediated recycling seems to be initiated from the *trans*-Golgi network. Together, this suggests that a recycling pathway operates at the level of the *trans*-Golgi linking directly to the ER. This pathway would be the preferred route for both toxins and resident Golgi proteins.

INTRODUCTION

Anterograde flow of material through the exocytic pathway is offset by the constant recycling of both proteins and lipids. This recycling helps to ensure that steady-state distributions of resident proteins are maintained within the pathway at the same time as keeping a lipid balance. Besides intra-Golgi recycling between cisternae (Hoe *et al.*, 1995; Love *et al.*, 1998; Lanoix *et al.*, 1999; Lin *et al.*, 1999), Golgi glycosylation enzymes also can recycle directly to the endoplasmic reticulum (ER). It is estimated that at least 5% of Golgi resident enzymes reside in the ER, at steady state (Pelletier *et al.*, 2000). This pool constitutes recycled material originating from the Golgi apparatus (Cole *et al.*, 1998; Storrie *et al.*, 1998).

The extent of ER recycling of Golgi resident membrane proteins is sufficient to allow for complete assembly of functional Golgi stacks. Thus, upon addition of nocodazole to depolymerize microtubules, the central and juxtanuclear Golgi apparatus relocates to the 100 or so peripheral ER exit sites scattered throughout the cell. This microtubule-independent relocation occurs in the absence of any detectable elements tracking outwards from the central Golgi apparatus. Rather, the Golgi apparatus undergoes a molecular deconstruction in the *trans*-to-*cis*-direction, i.e., resident glycosylation enzymes of the *trans*-cisternae/*trans*-Golgi network (TGN) relocate with faster kinetics than do enzymes of the *medial*-cisternae (Yang and Storrie, 1998). Enzymes seemingly enter the ER close to the microtubule organizing center (MTOC), diffuse through the ER, and then reemerge at peripheral ER exit sites. Here, Golgi stacks are then reassembled into discrete, yet fully functional Golgi stacks that remain in proximity to the ER exit site (Cole *et al.*, 1996). On repolymerization of microtubules, the 100 or so Golgi stacks move inwards toward the MTOC, reforming the Golgi ribbon.

The manner whereby Golgi resident proteins cycle through the ER is only partly understood. At least two mechanisms exist in mammalian cells that seem to operate in parallel. One is a well characterized signal-mediated recognition system that uses small C-terminal sorting signals, i.e., luminal KDEL or cytosolic K(X)KXX motifs. The KDEL signal is recognized by a receptor located at the *cis*-part of the Golgi stack. Both the receptor as well as resident proteins with K(X)KXX motifs are recognized and recycled via the COPI vesicle coat machinery. Indeed, the major component of the COPI coat, coatomer, binds directly to the K(X)KXX

Abbreviations used: BicD, Bicaudal-D; CGN, the *cis*-Golgi network; EEA1, early endosomal antigen-1; ER, endoplasmic reticulum; Gal-NAc-T2, *N*-acetylgalactosaminyltransferase-2; GalT, *β*-galactosyltransferase; GFP, green fluorescent protein; LAMP1, lysosomal associated membrane protein-1; Mann-II, *α*1,2-mannosidase II; MPR46, 46-kDa mannose-6-phosphate receptor; MTOC, microtubule organizing centre; p50, dynamitin; TfR, transferrin receptor; TGN, the *trans*-Golgi network; VTC, vesicular tubular carrier; *γ*-adaptin, adaptor protein-1 subunit *γ*.

motif. The second recycling mechanism allows Golgi resident proteins to continuously cycle through the ER (Girod *et al.*, 1999). This pathway is insensitive to perturbations of COPI and COPII function and hence named COP independent (for review, see Storrie *et al.*, 2000).

COPI-independent Golgi-to-ER recycling can be highlighted by preventing exit of proteins from the ER. Expression of GTP- or GDP-restricted mutants of the small GTPase Sar1p, required for COPII assembly and vesicle formation, effectively blocks COPII function. Under these conditions, most, if not all, Golgi resident proteins accumulate in the ER (Storrie *et al.*, 1998; Stroud *et al.*, 2003). The half-time for complete Golgi-to-ER recycling is in the order of 2 h, suggesting a slow flow of Golgi resident proteins through the ER. A slow recycling of Golgi resident proteins to the ER also can be induced by expression of GTP-restricted mutants of rab6A and rab33b, both small GTPases belonging to the rab family. Endogenous rab6 resides at the *medial/trans*-Golgi cisternae and in specialized cell types, in peripheral Golgi vesicular structures (Antony *et al.*, 1992), whereas rab33b resides at the *medial*-cisternae (Zheng *et al.*, 1998). Both rab6A (Martinez *et al.*, 1997; Girod *et al.*, 1999; White *et al.*, 1999) and rab33b (Valsdottir *et al.*, 2001) induce complete redistribution of Golgi markers into the ER and in terms of rab6A, relocation is thought to be microtubule dependent (Martinez *et al.*, 1997; White *et al.*, 1999). Indeed, a motor protein, rabkinesin6 (also termed RAB6-KIFL, MKlp2, KIF20A) has been shown to bind specifically to rab6 and is implicated in rab6 function. Of the two existing isoforms of rab6, A and A', only A binds to rabkinesin6 (Echard *et al.*, 2000, 2001). In apparent accordance with this, rab6A but not rab6A' redistributes the Golgi into the ER upon overexpression, suggesting a specific function of the rabkinesin6 motor complex in this process. Rab6A' on the other hand, seems to preferentially play a role in the recycling of material from the endocytic pathway through the TGN (Mallard *et al.*, 2002). The role of rabkinesin6 as a rab6A-specific effector during interphase was recently challenged by the finding that rabkinesin6 does not colocalize with rab6 and is only present in minute amounts in interphase cells. In contrast, rabkinesin6 is greatly up-regulated during mitosis where it plays a role in cytokinesis (Hill *et al.*, 2000; Fontijn *et al.*, 2001; Neef *et al.*, 2003). Nevertheless, the specific binding of rabkinesin6 to rab6A but not A' is consistent with the ability of rab6A but not A' to induce Golgi-to-ER recycling when overexpressed as a GTP-restricted mutant (Echard *et al.*, 2000). Both isoforms of Rab6 have been shown to interact directly with dynactin (Short *et al.*, 2002), a motor-binding complex and with Bicaudal-D (BicD) (Matanis *et al.*, 2002), a coiled-coil homodimer that interacts with several components of the dynein/dynactin complex (Hoogenraad *et al.*, 2001). This suggests an additional role for this motor complex in rab6 function. Indeed, overexpression of a carboxy-terminal domain of BicD that interacts with rab6, but not with cytoplasmic dynein, inhibits microtubule minus end-directed movement of green fluorescent protein (GFP)-rab6a vesicles. Under these conditions, rab6A and β-galactosyl-transferase (GalT), a *trans*-Golgi glycosylation enzyme, accumulate in peripheral structures (Matanis *et al.*, 2002). The relative role of rabkinesin6 and dynein/dynactin in COPI-independent Golgi-to-ER recycling remains unclear.

Here, we have investigated the relative contribution of rab6A and rab6A' in Golgi-to-ER recycling and the role played by the dynactin complex. We find that both rab6A and rab6A' GTP-restricted mutants can relocate from the Golgi to the ER and that both exert this through a microtubule-dependent process. We established that small interfering RNA (siRNA) knockdown of both rab6A and A' induces aberrant Golgi morphology and delays Golgi-to-ER recycling. Overexpression of one of the dynactin subunits, dynamitin (p50), or the carboxy-terminal domain of BicD, effectively inhibits rab6-dependent Golgi-to-ER redistribution. We also find that rab6 sequentially relocates the Golgi apparatus in a *trans*- to *cis*-manner much like that observed upon nocodazole treatment (Yang and Storrie, 1998). Given the *medial/trans*-Golgi localization of rab6 (Antony *et al.*, 1992), we suggest that both rab6A and A' functions through the dynactin complex at the *trans*-part of the Golgi, possibly where it intersects with the ER (Ladinsky *et al.*, 1999) and endosomes (Martinez *et al.*, 1994).

MATERIALS AND METHODS

Materials and Antibodies

All cell culture media and sera were obtained from Invitrogen (Carlsbad, CA). Restriction enzymes were purchased from New England Biolabs (Beverly, MA), and reagents for the purification of DNA purchased from QIAGEN (Valencia, CA). DNA primers were synthesized by Sigma-Aldrich (St. Louis, MO). Primary antibodies used were as follows: rabbit polyclonal to rab6 C-19 peptide (Santa Cruz Biotechnology, Santa Cruz, CA); sheep polyclonal to human TGN46 (Serotec, Oxford, United Kingdom); mouse anti-TGN38 (Affinity Bioreagents, Golden, CO); mouse monoclonal against human transferrin receptor (Zymed Laboratories, South San Francisco, CA); mouse monoclonal γ-adaptin (clone 100.3; Sigma-Aldrich); mouse monoclonal to early endosomal antigen-1 (EEA)-1 (BD Transduction Laboratories, Lexington, KY); lysosomal associated membrane protein-1 (LAMP1) (H4A3) monoclonal antibody (mAb) (Developmental Studies Hybridoma Bank, University of Iowa, Iowa City, IA); mouse monoclonal 9E10 recognizing the myc tag epitope (Covance, Berkeley, CA) and mouse anti-α-tubulin (DM1A; Sigma-Aldrich). Noncommercial antibodies used were rabbit anti-p24γ_3 (gp27; Fullekrug *et al.*, 1999), polyclonal anti-Sar1p antibody (Pepperkok laboratory; unpublished data), polyclonal anti-GFP (Karsenti laboratory; unpublished data) and from the following sources (given in parentheses): rabbit antisera to the cytoplasmic domain of human 46-kDa cation-dependent mannose 6-phosphate receptor (Annette Hille-Rehfeld, Gottingen University, Germany; Klumperman *et al.*, 1993); mouse monoclonal 53FC3 against mannosidase II (Graham Warren, Yale University, New Haven, CT; Burke *et al.*, 1983), rabbit anti-rat mannosidase II (Kelly Moremen, Georgia University, Athens, GA; Moremen and Touster, 1985), monoclonal anti-GalT (Ulla Mandel, Copenhagen University, Copenhagen, Denmark; Almeida *et al.*, 1999), sheep anti-GM130 (Francis Barr, MPI-Martinsried, Germany; published data), sheep antigolgin-84 (Martin Lowe, Manchester University, Manchester, United Kingdom; Diao *et al.*, 2003), rabbit anti-sec61β (Bernard Dobberstein, Heidelberg University, Heidelberg, Germany; High *et al.*, 1993), monoclonal 5B10 anti-rab6 (Angelika Barnekow, Muenster University, Muenster, Germany; Schiedel *et al.*, 1995), monoclonal 50.1 anti-dynamitin (Richard Vallee, Columbia University, New York, NY; Paschal *et al.*, 1993), and rabbit polyclonal anti-KAP3 (Tobias Stauber, European Molecular Biology Laboratory, Heidelberg, Germany; unpublished data). Secondary antibodies to sheep, rabbit, and mouse conjugated to Alexa-488, -568, -647, or -350 were obtained from Molecular Probes (Eugene, OR). Horseradish peroxidase-labeled secondary antibodies to rabbit and mouse were obtained from Jackson ImmunoResearch Laboratories (West Grove, PA).

Plasmids Used and Construction of pCMUIVmycp50

Rab6A-Q72L (GTP) and rab6A-T27N (GDP) were PCRed and subcloned into the *Bam*HI site of an optimized mammalian expression vector pCMUIV (Nilsson *et al.*, 1989) by using pGEM1Rab6AQ72L or T27N from Dr. Bruno Goud (Institut Curie, Paris, France) as a template source. Rab6A'Q72L and rab6A'T27N were similarly cloned into pCMUIV from pcDNA3.1HisRab6A'Q72L or T27N obtained from Dr. Francis Barr (Max-Planck-Institute, Martinsried, Germany). The primers used were previously reported in Girod *et al.* (1999). Phosphorylated enhanced green fluorescent protein (pEGFP)-Rab6AWT and pEGFP-Rab6A'WT were constructed by *Bam*HI digestion of pBS-Rab6AWT and pBS-Rab6A'WT previously generated from plasmids pFB372 and pFB343 donated from F. Barr. Each fragment was then subcloned into pEGFP-C1. Details of plasmid encoding Sar1p(H79G) are found elsewhere (Kuge *et al.*, 1994). Triple myc-tagged 120 amino acid C-terminal truncate of human BicaudalD2 (BicD-C amino acids 706 to stop codon) in pcDNA3.1/MycA (pFB1582-1) was also a kind gift of F. Barr. pCMUIVp50myc was constructed in the following way: flanking *Bam*HI sites and a Kosak consensus sequence were introduced using template cDNA from pCMVβp50myc (Echeverri *et al.*, 1996). Primers used for amplification were forward, 5'-TGATCCGGATCCGCCATGGCGGACCCTAAATAC; and reverse, 5'-TGATCCGGATCCTCAGTCCTCTTCAGAAATGAG. The resulting polymerase chain reaction (PCR) fragment was purified, digested with *Bam*HI, and

cloned into pCMUIV. Inserts of all plasmids received or constructed for this study were confirmed by sequencing both strands at least once.

Cell Lines and Microinjection

Wild-type HeLa and normal rat kidney (NRK) cells were grown in DMEM supplemented with 10% fetal bovine serum under standard tissue culture conditions. HeLa cells stably expressing tagged Golgi apparatus protein GalNAc-T2^{GFP} (Storrie *et al.*, 1998) or mannosidase II (Rabouille *et al.*, 1995) were maintained in the presence of 0.45 mg/ml G-418 sulfate. Purified plasmids were microinjected into the cell nuclei at 80 ng/μl by using an Eppendorf micromaniplulator and transjector and typically followed by 7-h expression time in a cell incubator unless otherwise specified. During microinjection cells were maintained at room temperature in CO_2-independent medium (minimal essential medium without phenol red but containing 30 mM HEPES; Invitrogen) and between 400 and 500 cells were injected per coverslip. The competition experiments involved sequential microinjection of BicD-C or mycp50 plasmid DNAs and preexpression for 24 h before rab6-GTP DNA injection and expression for 7 h. The nuclei of all cells in a defined marked area were injected in both sessions.

Transfection and RNA Depletion Experiments

Candidate siRNA sequences against each rab6 isoform simultaneously or individually were synthesized at QIAGEN. siRNA sequences targeting different regions of the rab6 gene common to both alternatively splice variants were A/A'-siRNA1: sense, 5'-GACATCTTTGATCACCAGAd(TT)-3' and A/A'-siRNA2: sense, 5'-CACCTATCAGGCAACAATTd(TT)-3'. For RNA interference against each isoform separately, the siRNA duplex sequences target within the alternatively spliced exon of the rab6 gene: A-siRNA: sense, 5'-GAGCGGTTCAGGAGCTTGAd(TT)-3' and A'-siRNA: sense, 5'-AGGCT-TCAGCTGTGGGATAd(CT)-3'. Control siRNA was a sequence provided by the manufacturers that has no significant homology to any mammalian gene. Cells were seeded at 30% confluence 36 h before transfection with siRNA by using Oligofectamine reagent (Invitrogen) according to manufacturer's instructions. Cells were transfected with 200 nM siRNA duplex and reseeded at 30% confluence onto coverslips in 24-well dishes. After 60 h, cells were treated a second time with siRNA and used after 92 h of total incubation with siRNA. The effectiveness of the siRNAs was ascertained by immunoblotting as described below and immunofluorescence with monoclonal and polyclonal anti-Rab6 antibodies that recognize both isoforms. To demonstrate the selectivity of the isoform-specific siRNA duplexes against the respective isoform of Rab6, HeLa cells were grown in six-well plates. They were treated once with the siRNAs as described above and after 22 h, transfected with 1 μg of plasmid encoding GFP-rab6A or GFP-rab6A' by using FuGene6 transfection reagent (Roche Diagnostics, Mannheim, Germany). After a further 28 h, the cells were prepared for SDS-PAGE as described below. Cell extracts were analyzed by 12% SDS-PAGE and anti-GFP immunoblot. To knock down KAP3 expression, HeLa GalNAc-T2^{GFP} cells grown on coverslips in six-well format were transfected with 200 nM siRNA duplex targeting human KAP3: sense, 5'-GTGTCGAGTTAGCTACAAAd(TT)-3' (Dharmacon Research, Lafayette, CO) by using Oligofectamine. After 48 h, the cells were microinjected with rab6-GTP–encoding plasmid as described above. Cells treated in parallel wells were scraped off in cell culture medium, centrifuged at low speed, washed in phosphate-buffered saline (PBS), and again centrifuged. The cell pellet was then lysed directly in Laemmli sample buffer. The supernatants were analyzed by 10% SDS-PAGE and anti-KAP3 immunoblot. Anti-α-tubulin was used as the loading control in all cases.

Nocodazole Treatment, Washout, and Live Cell Imaging

To depolymerize microtubules, HeLa GalNAc-T2^{GFP} cells grown in glass-bottom dishes (MatTek, Ashland, MA) were incubated with 10 μM nocodazole (Sigma-Aldrich) added to the normal growth medium for the stated time. Microinjection of DNA encoding the appropriate rab6 isoform mutant (A or A', GDP or GTP) was performed in the continued presence of nocodazole. To enable relocation of injected cells for live cell video microscopy, DNA was coinjected with a 1:10 dilution of dog IgG-Cy3. Cells were then returned to normal growth medium containing nocodazole and a CO_2 incubator for an expression period of 7 h up to 12 h. Using a PerkinElmer Ultraview RS spinning disk confocal laser microscope (Carl Zeiss, Jena, Germany) equipped with a temperature and CO_2 chamber, injected cells were located by the presence of dog IgG-Cy3 coinjection marker in the red emission channel. To study Golgi recovery in the presence of rab6-GTP, cells were washed at least 3 × 10 min with prewarmed drug-free imaging medium during noncontinuous recordings of GalNAc-T2^{GFP} in the green emission channel. Six to nine optical sections images were acquired every 20 min by using UltraView imaging software (Universal Imaging, Downingtown, PA). TIFF image stacks were assembled and averaged in NIH Image and processed in Adobe Photoshop.

Immunofluorescence Microscopy and Quantification

Paraformaldehyde fixed and 50 mM NH$_4$Cl quenched cells were permeabilized with saponin (0.05%) in the presence of 0.2% bovine serum albumin (BSA) in PBS for 5 min. Coverslips were then incubated in the same buffer with the appropriate primary antibodies. Cells were rinsed once in PBS (without BSA/saponin) and then incubated with secondary antibodies for 1 h in BSA/saponin. After two to three final rinses in PBS, coverslips were mounted on microscope slides in moviol. For triple stainings, sequential primary and secondary antibody stainings were carried out to avoid cross-species antibody reaction. Cells were viewed with a 63× objective on a Leica DM IRBE microscope by using a Hamamatsu charge-coupled device camera and Improvision OpenLab software. Semiquantitative analyses were carried out with the Measurements module by using raw digital images taken at constant exposure times predetermined to be subsaturating for the brightest samples. Outlines were drawn around each cell and the total fluorescence was determined by the mean pixel gray scale value of the region of interest. The measured fluorescence intensity values of rab6 versus the test inhibitory protein were plotted graphically for evaluation of the data.

RESULTS

Rab6A Predominantly Functions at the TGN Compartment

To test the relative effect of rab6 on marker proteins located at or near the *trans*-Golgi, we expressed rab6A Q72L (rab6A-GTP), a mutant known to accentuate rab6 function due to its much lower GTPase activity compared with wild type. HeLa cells were microinjected with 80 ng/μl plasmid DNA encoding rab6A-GTP and at 7 h postinjection, fixed and processed for indirect immunofluorescence by using antibodies recognizing rab6 and individual markers for the TGN or endosomal compartments. Cells labeled for TGN46, a mucin-like membrane protein originally identified as TGN38 in rat that cycles between the plasma membrane and the *trans*-Golgi, showed an ER-like redistribution in cells microinjected with rab6A-GTP (Figure 1A, cells marked with asterisks): a perinuclear staining combined with reticular structures pervading the entire cytoplasm. Noninjected cells revealed the anticipated compact juxtanuclear pattern typical of the Golgi apparatus. In contrast, cells labeled for the small mannose-6-phospate receptor (MPR46) (Figure 1B), transferrin receptor (TfR) (Figure 1C), or the adaptor protein-1 subunit γ (γ-adaptin) (Figure 1D) showed accumulation in distinct peripheral structures (arrows) upon rab6A-GTP expression and a complete loss of juxtanuclear staining. The applied markers MPR46, TfR, and γ-adaptin are proteins of the dynamic endosomal/*trans*-Golgi network although the steady-state distribution of these proteins is in the perinuclear region. Golgi enzymes and TGN46 did not accumulate in the peripheral clusters at the membrane tips (see below), suggesting these sites contain membranes of endosomal origin. Cells labeled for the endosomal rab-5 effector protein, EEA1 (Figure 1E) showed a partial effect on the distribution of the endosomal-like punctate vesicular staining, with a shift from a relatively juxtanuclear to a more scattered pattern upon rab6A-GTP expression. EEA1-positive structures in rab6A-GTP–expressing cells also were enlarged compared with neighboring control cells. For each protein marker used, more than 100 rab6A-GTP–expressing cells were inspected. In the case of TGN46, ~75% of rab6A-GTP–expressing cells showed complete redistribution of TGN46 to the ER after 7 h. The extent of redistribution was seen to correlate with the level of rab6A-GTP in the cell as judged by staining with anti-rab6 antibody. In the case of MPR46, TfR, and γ-adaptin, ~75% of rab6A-GTP–expressing cells lacked perinuclear staining and clusters at the tips of membrane protusions could be seen in 30–40% of rab6A-GTP–expressing cells. Rab6A-GTP affected the early endosome compartment in >30% of cells. In contrast to these perinuclear localized markers, the steady-state distribution of the late endosomal/early lysosomal marker protein, LAMP1 was not affected by rab6A-GTP expression (Figure 1F). Further-
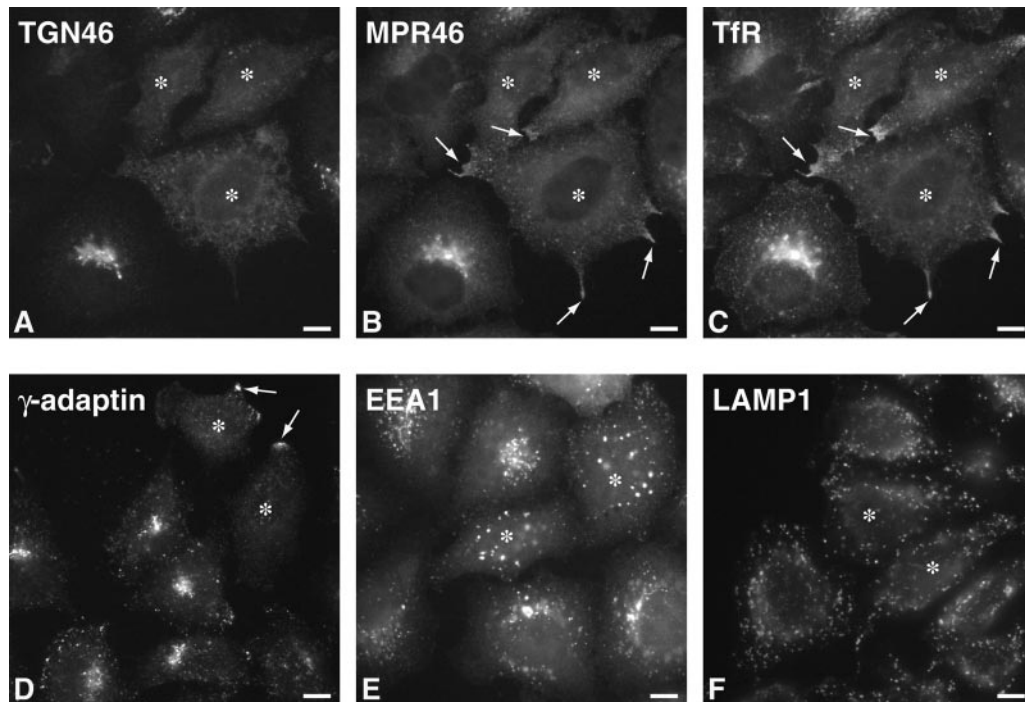
Figure 1. Overexpression of rab6A disrupts the steady state of the TGN and perinuclear recycling compartments. HeLa cells expressing rab6A-GTP (asterisks) were analyzed by immunofluorescence microscopy by using antibodies to the indicated endogenous proteins. Noninjected cells serve as an internal control. (A–C) Cells were triple immunostained for TGN46, MPR46, and TfR. In rab6A-GTP–expressing cells (asterisks), TGN46 redistributed to an ER-like reticulum (A), whereas MPR46 and TfR colocalized in accumulations at extreme peripheral points of the cell (arrows in B and C). (D) Similarly to MPR46 and TfR, γ-adaptin also redistributed to these peripheral points. (E) In response to rab6A-GTP overexpression, early endosomes defined by the nonrecycling protein EEA-1 were found to be slightly larger and abnormally distributed away from the juxtanuclear region compared with the situation in control cells. (F) In contrast, rab6A-GTP had no effect on the late endosome/lysosome compartment defined by LAMP1 antibody staining. Bars, 10 μm.

more, expression of the constitutively GDP bound mutant of rab6A, T27N (rab6A-GDP) did not affect the steady-state distribution of TGN46, γ-adaptin, or MPR46 (our unpublished data). Together, this suggests that under the same conditions that perturb Golgi-to-ER recycling, rab6A also affects proteins that cycle between the *trans*-Golgi and the plasma membrane (TGN46) and the *trans*-Golgi and recycling and early endosomes (MPR46, γ-adaptin, and TfR), without affecting late endosomal and lysosomal compartments (LAMP1).

In terms of Golgi-to-ER recycling, membranes and proteins of the Golgi can either pass sequentially back from cisternae to cisternae via COPI vesicles and/or conceivably, directly from the *trans*-Golgi to the ER (Storrie *et al.*, 2000). To distinguish between these two routes in respect to rab6, we looked at the relative disappearance of *cis*-, *medial*-, and *trans*-Golgi resident integral membrane proteins at intermediate times after expression of rab6A-GTP. This analysis was initially performed in NRK cells because suitable antibodies against endogenous rat Golgi proteins were available for immunofluorescence. Importantly, comparable and readily detectable levels of each Golgi protein were obtained with these antibodies under the same camera exposure settings making a direct comparison feasible. Hence, NRK cells were injected with plasmid DNA encoding rab6A-GTP and fixed at 4 or 6 h to reveal intermediate states of partial dissolution of the Golgi apparatus (Figure 2, compare double-labeled cells marked with arrows). As can be seen, rab6A-GTP preferentially redistributed the *trans*-marker TGN38 to the ER before p24γ₃ (Figure 2A), a member of the p24 family of small transmembrane proteins that cycles between the ER

and the *cis*-face of the Golgi apparatus (Fullekrug *et al.*, 1999) and before the *medial*-marker α1,2-mannosidase II (Mann-II) (Rabouille *et al.*, 1995) (Figure 2B). Mann-II in turn was redistributed before p24γ₃ (Figure 2C). TGN38 staining also was lost before giantin and GM130, two markers of the *cis*-Golgi network (CGN) (Figure 2, D and F). Similarly to TGN38, the *trans*-Golgi marker GalT lost its juxtanuclear Golgi staining before giantin (Figure 2E). When comparing Mann-II or Golgin 84 with GM130, we saw a more rapid disappearance of the two more *medial*-markers (Rabouille *et al.*, 1995; Diao *et al.*, 2003; Satoh *et al.*, 2003) than with the CGN/*cis* marker GM130 (Figure 2, G and H). It thus seems that Rab6 induces a Golgi-to-ER redistribution that occurs progressively with the *trans*-most cisternae disappearing first followed by the *medial*-cisternae and finally, the *cis*-cisternae and the CGN, similar to previous observations made during nocodazole experiments (Yang and Storrie, 1998). Given its subcellular localization, it is likely that rab6 predominantly operates from the level of the *trans*-Golgi, possibly where the secretory pathway intersects with the ER and the endocytic pathway, the former through the observed direct interdigitation between *trans*-cisternae and the latter through proximity to the *trans*-part of the Golgi.

Rab6-GTP Redistributes the Golgi to the ER in a Microtubule-dependent Manner

Given the similarity between rab6-GTP and nocodazole induced relocation with respect to the *trans*-part of the Golgi preceding earlier cisternae, we tested for the dependency of rab6A-GTP–induced Golgi-to-ER relocation on microtu-
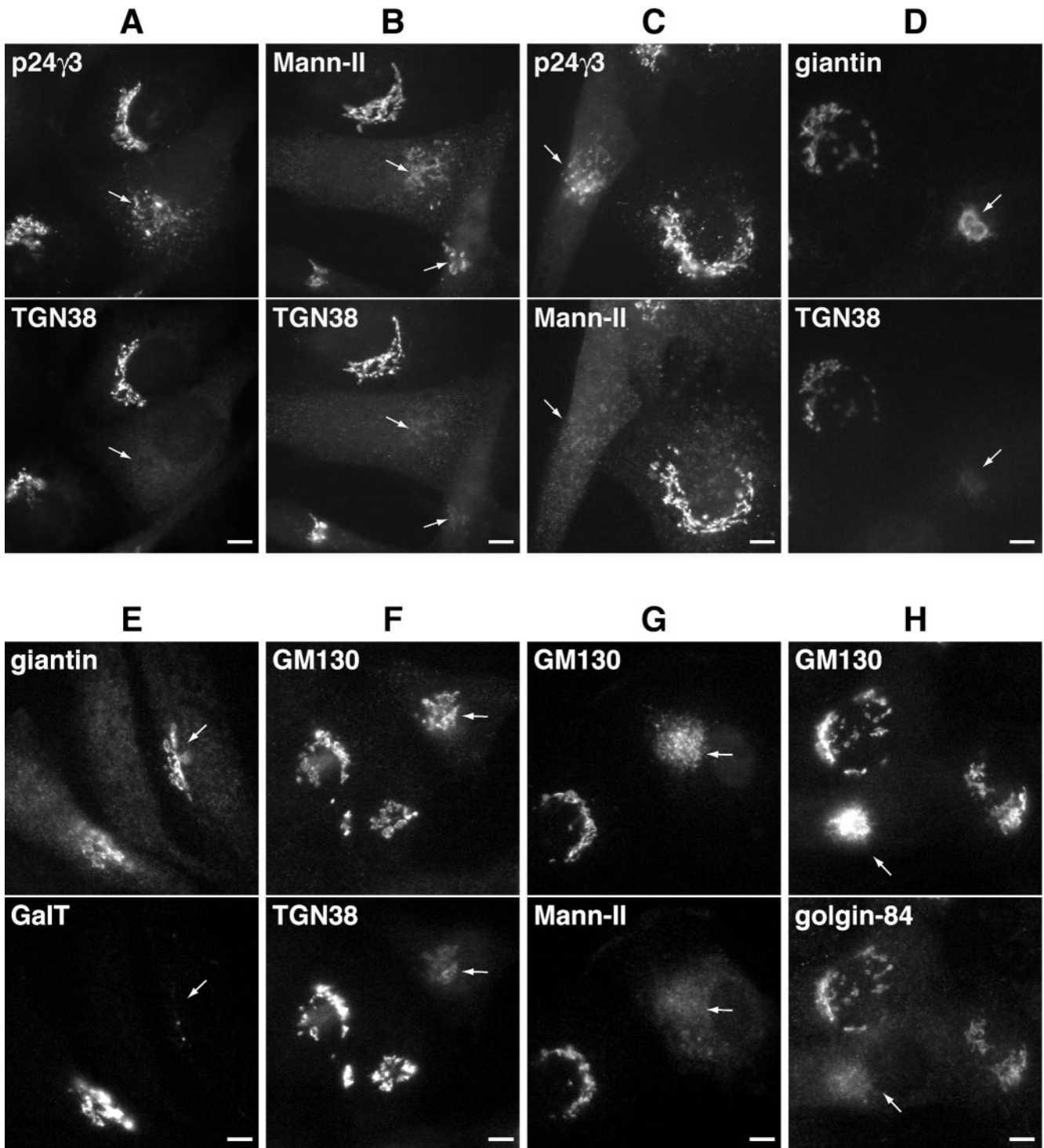
Figure 2. The TGN is most sensitive to redistribution by rab6A-GTP. To delineate the kinetics of Golgi redistribution by rab6, double-label immuno-fluorescence was carried out on NRK cells 4–6 h postinjection of DNA encoding rab6A-GTP. Retrograde movement seemed to occur in a stepwise redistribution occurring from TGN to *medial*- to *cis*-Golgi. Arrows indicate cells in which a sequential redistribution can be seen. Thus, rab6A-GTP stimulated the initial disappearance of immunostaining for TGN38 before p24γ3, which resides in the *cis*-Golgi (A) and before *medial/trans*-localized glycosyltransferase Mann-II (B). Consistent with this, Mann-II also was redistributed before p24 γ3 (C). Similarly, TGN38 and GalT staining disappeared before giantin (D and E). TGN38 (F), MannII (G), and golgin-84 (H) all redistributed before the *cis*-Golgi marker GM130. Bars, 10 μm.

bules. We asked whether rab6 could redistribute the Golgi enzyme *N*-acetylgalactosaminyltransferase-2 fused to GFP (GalNAc-T2^{GFP}) to the ER in the absence of microtubules.

This enzyme distributes across the Golgi stack (Rottger *et al.*, 1998). Cells were pretreated with nocodazole for 5 h, micro-injected with DNA encoding rab6A-GTP, and assayed after
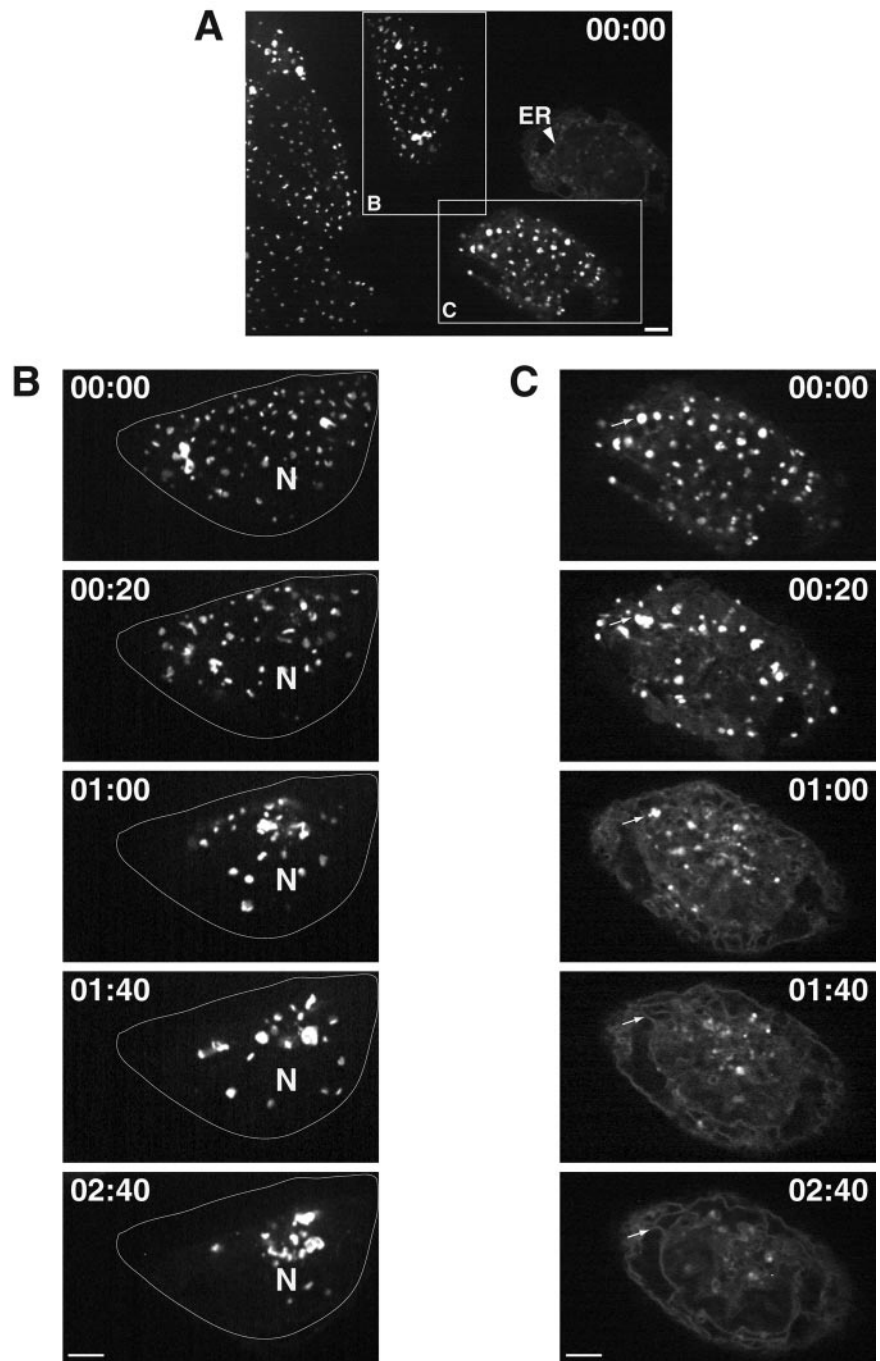
Figure 3. Dynamics of Golgi fragments in rab6A-GTP–expressing cells after nocodazole removal. Time-lapse images (time indicated in hours:minutes) show the initial pattern of dispersed Golgi fragments in nocodazole-treated GalNac-T2^{GFP} stably transfected HeLa cells and their movement upon the repolymerization of microtubules in the presence and absence of rab6A-GTP. (A) Rab6A-GTP–expressing cells (box C) show a similar pattern of scattered Golgi elements as in control cells (box B) at t = 0. A few cells with particularly high levels of rab6A-GTP show partial localization of GalNAc-T2^{GFP} in the ER as well as in mini-Golgi (arrowhead). This shows that rab6-directed Golgi-to-ER transport can occur in the absence of microtubules but only inefficiently. (B) During nocodazole washout in control cells, the scattered Gal-NAc-T2^{GFP} labeled Golgi fragments cluster (t = 20 min) and net movement is inward (t = 1h) toward the juxtanuclear region denoted by N. After 2 h 40 min of incubation without nocodazole, most Golgi fragments are concentrated at the cell center. The outline indicates the cell periphery (C) In rab6-GTP–expressing cells, there is no recovery of the Golgi apparatus. Rather, the Golgi fragments (arrows) partially regroup (t = 20 min) but then melt into the underlying ER network, which becomes increasingly distinct (t = 1 h to 2 h 40 min). Bars, 10 μm.

6 h of plasmid expression in the continued presence of nocodazole for GalNAc-T2^{GFP} redistribution. At 5 h of nocodazole treatment, the juxtanuclear Golgi apparatus is completely relocalized to peripheral ER exit sites as individual Golgi stacks. These peripheral Golgi stacks are functionally normal in terms of enzyme processing, transport, and constitutive recycling of resident proteins with the ER (Storrie et al., 1998). Cells were then microinjected with rab6A-GTP to see whether GalNAc-T2^{GFP} would now redistribute to the ER. After 6 h of rab6A-GTP expression, we observed in a small proportion of rab6-expressing cells (10%), an intermediate phenotype where GalNAc-T2^{GFP} had partially redistributed to the ER with continued localization in mini-

Golgi structures. A representative example of this is shown in Figure 3A (arrowhead). The majority of rab6A-GTP–expressing cells (outlined and labeled as C in Figure 3A), however, showed a pattern of scattered Golgi similar to that observed in the absence of rab6A-GTP (outlined and labeled as B in Figure 3A). Thus, nocodazole treatment inhibits rab6A-GTP from redistributing the Golgi to the ER. To confirm that microtubules were indeed needed for Golgi-to-ER transport, we washed out the nocodazole and monitored GalNAc-T2^{GFP} movement in living cells by time-lapse microscopy. In control cells (Figure 3B), peripheral Golgi stacks moved toward the cell center where they regained their juxtanuclear appearance. This most likely occurred along

reassembling microtubules (Ho *et al.*, 1989). In contrast, cells expressing rab6A-GTP (Figure 3C) showed a steady increase in tubular-reticular and perinuclear staining concomitant with the disappearance of fluorescent Golgi elements containing GalNAc-T2^{GFP} (arrows), suggesting that GalNAc-T2^{GFP} had relocated into the ER. The peripheral Golgi elements in rab6A-GTP–expressing cells retained their ability to locally fuse with each other as they moved toward the juxtanuclear region, similar to the behavior of Golgi elements in control cells before their final reclustering in the centrosomal region. However, the majority of such Golgi membranes seemed to merge with the ER before reaching a peri-centrosomal location (arrows). This process was completed within 2 h 40 min after nocodazole washout. In additional experiments, we determined that the speed of redistribution of GalNAc-T2^{GFP} to the ER correlated with the level of rab6A-GTP expression in the cell. With the highest levels of rab6A-GTP expression representing ~20% of the injected cell population, a complete ER fluorescence of GalNAc-T2 ^{GFP} was achieved already after 20 min after the nocodazole washout (our unpublished data).

The inability of rab6A-GTP to relocate GalNAc-T2^{GFP} in the absence of microtubules is not explained by the fact that Golgi stacks are located at peripheral ER exit sites. Golgi-to-ER recycling still takes place in nocodazole-treated cells as evidenced by earlier studies where a portion of the peripheral Golgi stacks were bleached and then monitored for fluorescent recovery by using the same cell line expressing GalNAc-T2^{GFP} (Storrie *et al.*, 1998). In that same study, an ER exit block induced by overexpression of GTP-restricted Sar1p mutant, resulted in the gradual disappearance of GalNAc-T2^{GFP} from mini-Golgi and its subsequent appearance in the ER. Thus, the Golgi is still directly connected to the underlying ER in the absence of microtubules and it is not that Golgi-to-ER recycling was inhibited, per se, but that rab6 as a regulator of Golgi-to-ER transport had been rendered nonfunctional in the absence of microtubules.

Both rab6A and rab6A' Stimulate Golgi-to-ER Transport

The observed dependency for intact microtubules during rab6-dependent recycling prompted us next to compare the two isoforms of rab6, rab6A and rab6A'. The two isoforms differ in three amino acids, making them functionally distinct in that rab6A binds the motor protein rabkinesin6, whereas rab6A' does not (Echard *et al.*, 2000, 2001). Rab6A'-GTP was expressed and compared with rab6A-GTP for the ability to relocate various Golgi enzymes to the ER. As shown in Figure 4A, microinjection of 80 ng/μl plasmid encoding rab6A or A' induced a complete relocation of GalNAc-T2^{GFP} to the ER in 60 $\pm$ 15% of cells within 7 h of expression (arrows). To verify that rab6-GTP indeed redistributes Golgi enzymes to the ER, we performed colocalization of GalNAc-T2^{GFP} with the residential ER protein sec61β. The double immunofluorescence images show good colocalization of both proteins giving rise to typical perinuclear and cytoplasmic ER staining (Figure 4D). The same experiment was performed in HeLa cells stably expressing Mann-II fused to an 11-amino acid epitope VSV-G (Mann-II^{VSV}; Rabouille *et al.*, 1995). This Golgi marker also was completely relocated into the ER in rab6A- and rab6A'-expressing cells as evidenced by perinuclear staining (Figure 4B, arrows). Immunostaining for endogenous GalT also was performed and again no qualitative difference could be observed when comparing the GTP-restricted mutants of rab6A and A' (our unpublished data). Rab6A'-GTP also redistributed recycling proteins of the perinuclear endosomal compartment such as TfR to the periphery of cells in a

way that was indistinguishable from rab6A-GTP (our unpublished data). That rab6A' could function in Golgi-to-ER transport at all was surprising given previous reports emphasizing a role for this rab protein in endosome-to-Golgi transport but not in Golgi-to-ER transport (Echard *et al.*, 2000).

To avoid the possibility that excessive amounts of rab6A'-GTP may cause nonspecific interactions with rab6A effectors, we performed careful quantitative experiments at low plasmid concentrations (20 ng/μl). Each plasmid DNA was injected into HeLa cells expressing GalNAc-T2^{GFP} on separate scratched regions of a coverslip. At 7 h postinjection, the cells were fixed and stained with anti-rab6 antibody recognizing both isoforms. Each expressing cell was then quantified for the level of rab6 protein as described in *Materials and Methods* and classed into three categories based on the localization of GalNAc-T2^{GFP}: 1) "Golgi" with predominant fluorescence of GalNAc-T2^{GFP} in the Golgi, 2) "intermediate" with Golgi and ER GalNAc-T2^{GFP} fluorescence, and 3) "ER" with GalNAc-T2^{GFP} located exclusively in the ER. Each category of phenotype can be visualized in Figure 4A (Golgi, G; intermediate, arrowhead; ER, arrow) for both rab6A- and A'-injected cells and correlates with the amount of rab6 expressed in each cell. When cells were scored and compared quantitatively in this manner, no difference was revealed between rab6A-GTP and rab6A'-GTP (Figure 4C). The percentage of cells expressing a level of protein capable of redistributing GalNAc-T2^{GFP} completely to the ER (23 and 31%), partially to the ER (13 and 11%), or not at all to the ER (65 and 58%) also was the same for rab6A and A'. Thus, the same level of rab6A'-GTP protein was as effective as rab6A-GTP in redistributing Golgi cisternae either fully or partially to the ER.

To obtain independent experimental evidence for a role of rab6 in on Golgi-to-ER recycling, we also performed RNA interference experiments removing endogenous rab6 from the cells (Figure 5). Control siRNA and siRNAs targeting rab6A or A' or both isoforms simultaneously were used. The specificity of each oligonucleotide is demonstrated in Figure 5, A and B. Two different antibodies generated against rab6 revealed that most of the endogenous rab6 had been removed after repeated transfection of rab6 (A/A') siRNAs over a 4-d period (see first two lanes in Figure 5A). Using siRNA targeting both rab6A and rab6A' (A/A'-siRNA1, A/A'siRNA2), we observed a marked decrease compared with cells transfected with control siRNAs (Figure 5, lanes 3 and 4 compared with lane 5). The specificity of siRNAs targeting rab6A or rab6A' individually (A-siRNA, A'-siRNA) were tested through their ability to inhibit expression of rab6A or rab6A' fused to GFP (Figure 5B). As can be seen, A/A'-siRNA1 and A/A'-siRNA$_2$ inhibited both GFP-rab6A as well as GFP-rab6A' expression (lanes 1, 2 and 6, 7), whereas A-siRNA only inhibited GFP-rab6A but not GFP-rab6A' expression (compare lane 3 with 8). Conversely, A'-siRNA only inhibited GFP-rab6A' expression but not GFP-rab6A (compare lane 9 with 4). Finally, cells treated with an unrelated control siRNA did not affect levels of expression from GFP-rab6A or GFP-rab6A' plasmids as expected.

We next examined the Golgi morphology of different Golgi markers in the siRNA-treated cells. Shown in Figure 5, G–J, is the different effect of A-siRNA, A'-siRNA, and A/A'-siRNA1 on the stably expressed GalNAc-T2^{GFP}. Only when removing endogenous rab6A and A' (Figure 5F) did we observe a marked difference on the pattern of GalNAc-T2^{GFP}. Rather than observing a typical ribbon- and Golgi-like juxtanuclear staining normally associated with GalNAc-T2^{GFP} (Figure 5, G–I), we observed a few condensed and
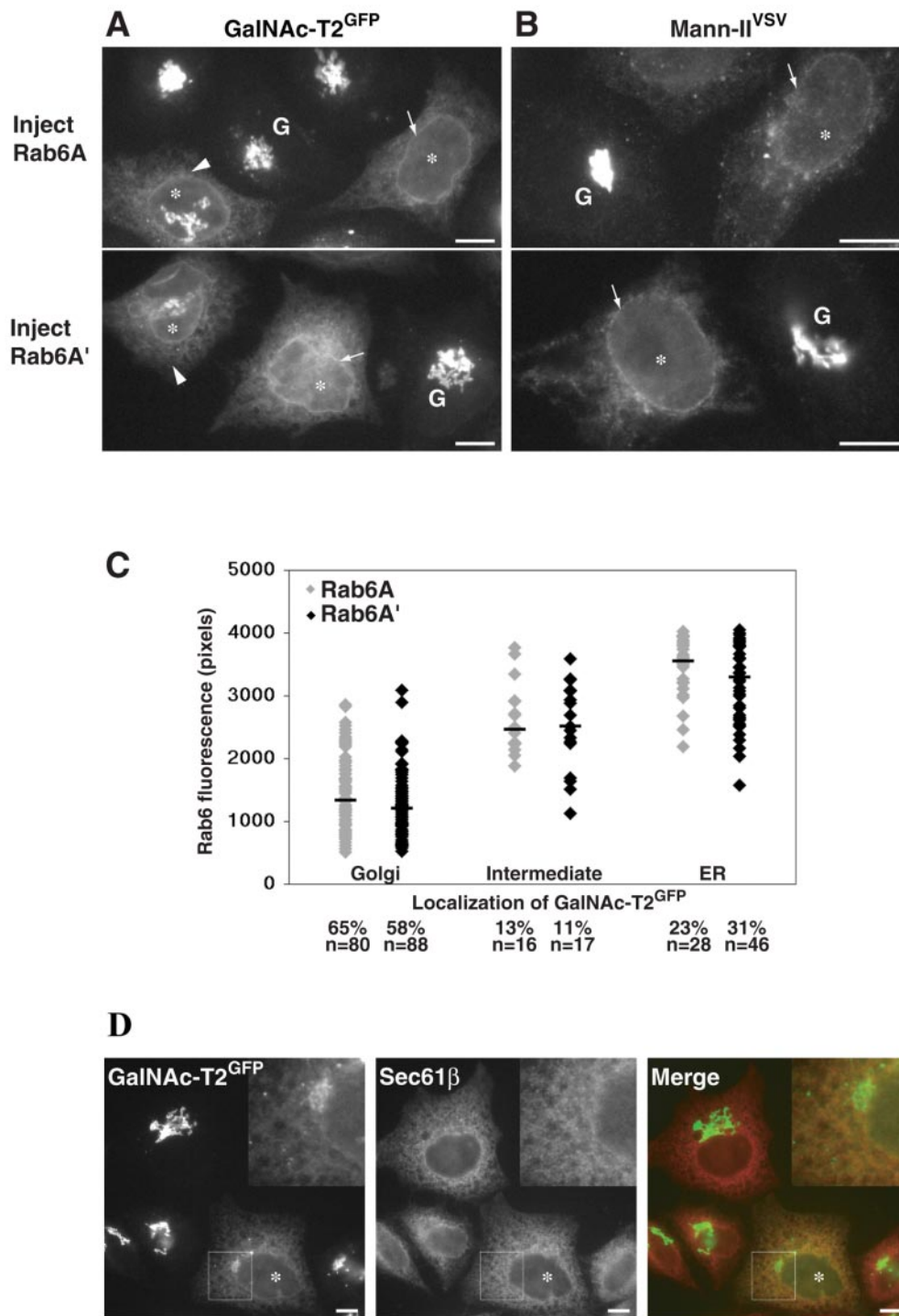
Figure 4. Both rab6A′ and rab6A induce transport of Golgi enzymes to the ER, despite that rab6A′ does not bind rabkinesin6. HeLa cells stably expressing GalNAc-T2^{GFP} (A) or Mann-II^{VSV} (B) were injected with 80 ng/μl DNA encoding isoform rab6A-GTP or rab6A′-GTP and incubated for 7 h at 37°C. Cells were then fixed and labeled by indirect immunofluorescence for rab6 and Mann-II or in the case of GalNAc-T2^{GFP}, which can be visualized directly, only with rab6. Both rab6A-GTP– and rab6A′-GTP–expressing cells (asterisks) showed the ability to completely redistribute GalNAc-T2^{GFP} or Mann-II normally located in the Golgi (G) to the ER (arrows). An example of an intermediate phenotype used in the scoring presented below is indicated (arrowhead). (C) HeLa GalNAc-T2^{GFP} cells were injected in two separate regions on a scratched coverslip with 20 ng/μl DNA encoding rab6A-GTP or rab6A′-GTP. After 7 h of expression time, cells were fixed and immunostained with anti-rab6 antibodies that recognize both isoforms. Total rab6 fluorescence from individual cells (in arbitrary units) was measured using OpenLab software as indicated in *Materials and Methods* and plotted on the *y*-axis. The plot shows the correlation of expression level with the resulting phenotype which was categorized based on the redistribution pattern of the Golgi marker GalNAc-T2^{GFP} in that cell. Each dot represents the measurement from a single cell; the bar represents the median expression level from all cells within a classification. The number of cells in each category is expressed as a percentage, and the number of counted microinjected cells is indicated (n). (D) Cells microinjected with a rab6A-GTP–encoding expression plasmid were fixed and immunostained with the ER marker sec61β and viewed for GalNAc-T2^{GFP}. In the "Merge" image, orange indicates colocalization of sec61β and GalNAc-T2^{GFP}. Bars, 10 μm.
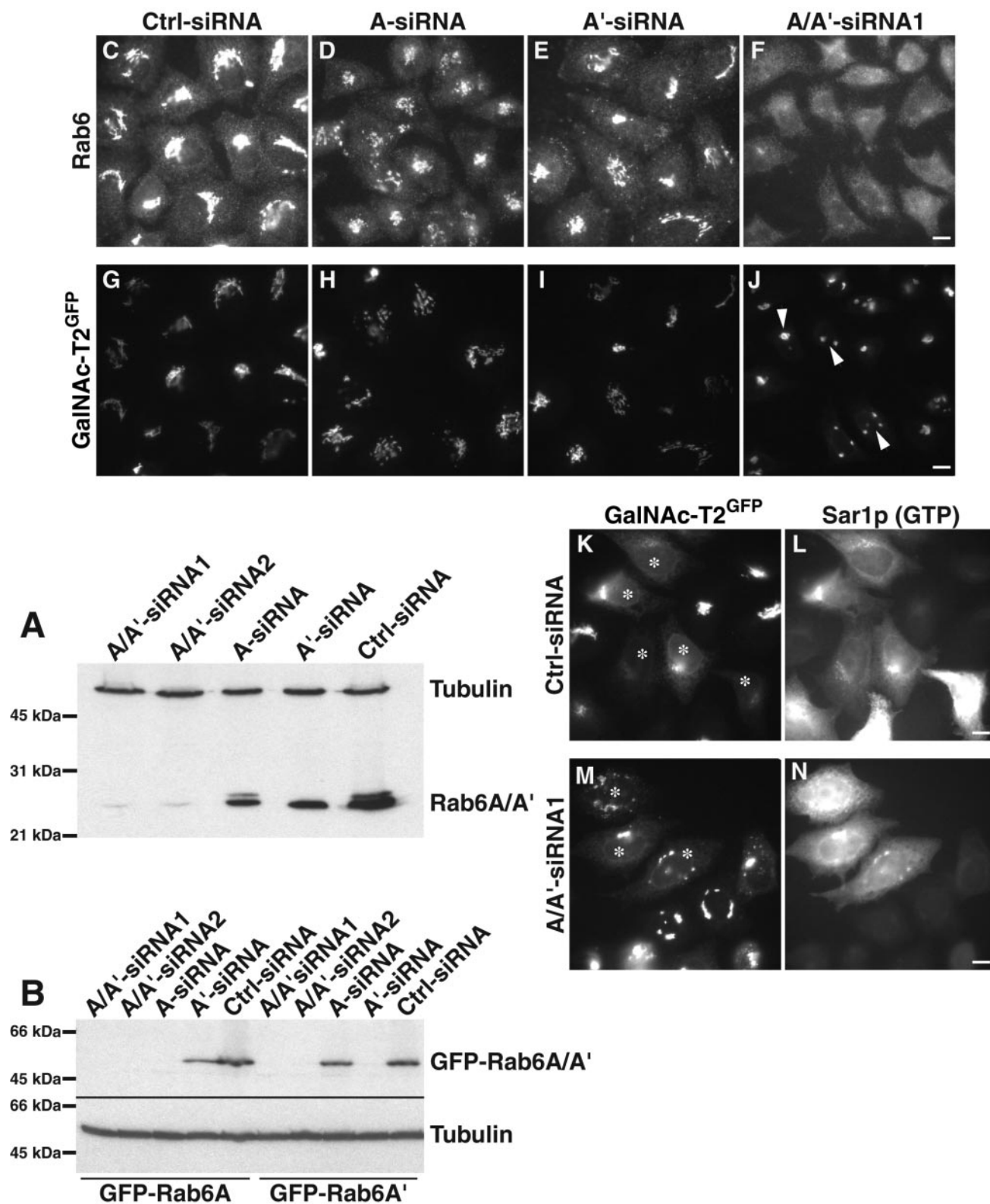
Figure 5. Reduction of both rab6A and A′ by RNA interference (RNAi) effects Golgi structure and transport. (A) Western blot demonstration of reduced total rab6 protein levels by two different siRNA sequences (labeled A/A′-siRNA1 and 2) or reduced rab6A or A′ protein upon addition of the respective isoform-specific duplex (labeled A-siRNA and A′-siRNA). Whole cell extracts were prepared 92 h after repeated transfection with the appropriate siRNA and analyzed by Western blotting with anti-rab6 mAb. Levels of rab6 in cells treated with control-siRNA (Ctrl-siRNA), and levels of α-tubulin were not affected. (B) Suppression of individual rab6 isoforms by isoform-specific siRNA sequences. Cells treated with siRNA for 22 h were transiently transfected with plasmids encoding GFP-rab6A or GFP-rab6A′ and prepared for immunoblot 28 h postplasmid transfection. The anti-GFP immunoblot shows the efficiency and specificity of each siRNA under these

brighter Golgi structures (Figure 5J), suggesting either a loss of Golgi volume and/or an increased concentration of Gal-NAc-T2^{GFP} in a smaller region of the Golgi. Similar results were obtained when A/A'-siRNA2 was used (our unpublished data). Other Golgi marker proteins including GM130 and TGN46 also displayed an unusually compact Golgi morphology (Supplementary Material Figure 1). Only a minor effect was observed when staining for M6PR (Supplementary Material Figure 1) and TfR (our unpublished data). Cells transfected with A-siRNA or A'-siRNA showed no obvious affect at the visual level on either GalNAc-T2^{GFP} (Figure 5, H and I), GM130, TGN46, or MPR46 (Supplementary Material Figure 1), suggesting that the condensed Golgi-like staining patterns seen for the different Golgi markers requires the removal of both rab6A and A'.

We next tested the effect of removal of rab6A and A' on Golgi-to-ER recycling. Cells were transfected with A/A'-siRNA1 twice over 92 h and microinjected with plasmid expressing the GTP-restricted mutant of Sar1p to block ER export. Cells transfected with control siRNA revealed an ER-like GalNAc-T2^{GFP} staining after expression of Sar1p-GTP with only a faint staining of remaining Golgi remnants (Figure 5, K and L). Cells not expressing Sar1p-GTP showed a normal Golgi pattern and no obvious ER staining. In contrast, cells transfected with the A/A'-siRNA and expressing Sar1p-GTP still showed an aberrant Golgi morphology similar to neighboring noninjected cells with some ER staining (Figure 5, M and N). This suggests that in cells with rab6A and rab6A' knockdown Sar1p-GTP is less effective in relocalizing the Golgi to the ER. We only observed this inhibitory effect at early time-points (3–4 h after injection of the Sar1p-GTP coding plasmid). By later time points of Sar1p-GTP expression (8 h) cells, which received A/A'-siRNA1, showed GalNAc-T2^{GFP} fully redistributed to the ER with no distinction to cells which received control siR-NAs (our unpublished data). This ability of A/A'-siRNA1 to "slow down" Golgi-to-ER recycling is consistent with the notion of rab6 being a regulator of Golgi-to-ER recycling.

Figure 5 (cont.) conditions. Thus, each GFP-rab6 isoform is not expressed when targeted by its siRNA and is expressed when incubated with siRNA against the other isoform. siRNA targeting both rab6A and A' inhibited expression from GFP-rab6A and GFP-rab6A' plasmids as expected. GFP-rab6 expression in cells treated with an unrelated control siRNA and α-tubulin were not affected. (C–J) Immunofluorescence images of cells expressing the Golgi marker GalNAc-T2^{GFP} after double treatment with the corresponding siRNAs for 92 h and immunostaining with rabbit anti-rab6 antibody. These illustrations were imaged with the same camera exposure settings, allowing a direct comparison of rab6 levels after RNAi treatment (C–F). The minor effect of reduced levels of rab6A (D and H) or A' (E and I) on Golgi structure. Reduction of rab6A and A' combined (F and J) affects overall Golgi morphology compared with control-treated cells (C and G). Arrowheads indicate the cells in which there was a major reduction in Golgi size. (K–N) Relocalization of GalNAc-T2^{GFP} to the ER after the introduction of Sar1p (GTP) is delayed in rab6 knockdown cells. Stably transfected GalNAc-T2^{GFP} cells treated with Ctrl-siRNA (K and L) or A/A'-siRNA1 (M and N) for 92 h were injected with DNA encoding dominant negative Sar1p (asterisks) and incubated for 4 h. Cells were then processed for double labeling with antibodies directed against rab6 (our unpublished data) and Sar1p (L and N) and observed by microscopy. Cells were analyzed for the amount of GalNAc-T2^{GFP} redistribution (K and M). Bar, 10 μm.

Rab6-directed Golgi-to-ER Transport Is Dependent on BicD and the Dynactin Complex

That rab6 would exert its effect on Golgi to ER transport as a regulator is consistent with the observation that rab6A interacts with the motor protein rabkinesin6 and that rab6-GTP requires microtubules for the redistribution of Golgi markers to the ER (Martinez *et al.*, 1997; this study). However, both rab6A-GTP and rab6A'-GTP affects the redistribution of Golgi markers to the ER equally well, and the removal of both is required for an adverse effect on Golgi staining of several Golgi markers. This points to a very similar role of rab6 A and A', if not identical, in terms of acting as regulators of Golgi-to-ER recycling. As only rab6A but not rab6A' interacts with rabkinesin6, another motor protein is likely to operate in Golgi-to-ER recycling in conjunction with rab6A'.

Another kinesin implicated in trafficking between the Golgi and ER is KIF3, which localizes to Golgi-related compartments (Le Bot *et al.*, 1998). This heterotrimeric kinesin was recently discovered to interact with dynactin through its cargo-binding subunit KAP3 (Deacon *et al.*, 2003), indicating controlled coupling between anterograde transport and retrograde recycling. To test whether KIF3 serves as a motor protein in rab6 directed Golgi-to-ER transport, we disrupted this kinesin in the GalNAc-T2^{GFP} stable expressing HeLa cell line by using siRNA directed specifically against KAP3 mRNA. As shown in Figure 6A, quantitative scanning from Western Blots of cell lysates probed with anti-KAP3 antibody showed that KAP3 protein depletion was 83% after 48 h of siRNA treatment, compared with the mock-treated cells. However, 7 h after microinjection of rab6A-GTP–expressing plasmid, the KAP3 knockdown cells showed the same degree of Golgi redistribution of GalNAc-T2^{GFP} to the ER as in control cells (Figure 6B). MPR46 also was redistributed by rab6A-GTP to the tips of KAP3 knockdown cells as in control cells (our unpublished data). Together, the KIF3 motor complex does not seem to be an effector in the rab6-induced redistribution event. We next examined whether dynactin is involved.

The recent discovery that both rab6A and A' interact with dynactin (Short *et al.*, 2002) and BicD (Matanis *et al.*, 2002) makes this motor-binding complex a potential candidate for Golgi-to-ER recycling. Both proteins are more typically known for their involvement in minus end-directed transport through association with the microtubule motor dynein (Hoogenraad *et al.*, 2003). BicD also localizes to the *trans*-Golgi and with dynactin at microtubule plus ends. The functional relevance of these interactions in relation to rab6 function, however, has not been explored. The only functional link is that overexpression of a C-terminal rab6-binding fragment of BicD seemingly blocked minus end-directed movement of intracellular structures visualized by rab6-GFP (Matanis *et al.*, 2002). It was therefore of interest to directly test the role of BicD within microtubule- and rab6-dependent Golgi-to-ER transport. We used the same C-terminal domain of BicD (BicD-C) as described in the previous study. The BicD-C fragment competitively displaces endogenous BicD from its limited number of binding sites at the *trans*-Golgi but lacks the dynein interaction domain. It retains its ability to bind dynamitin, a subunit of the dynactin complex and rab6 (Karki and Holzbaur, 1995; Hoogenraad *et al.*, 2001). DNA encoding BicD-C was microinjected into cells expressing the Golgi marker GalNAc-T2^{GFP} in a defined region of a coverslip and preexpressed for 24 h. This was subsequently followed by microinjection of DNA encoding rab6A-GTP into the same cells. After 7 h, the cells were fixed

and stained for BicD-C and rab6. The levels of expression of BicD-C and rab6 were evaluated in each individual cell by quantification of fluorescence intensity from digital images as described in *Materials and Methods*. Graphical representation of the expression levels (Figure 7A) revealed that cells expressing high levels of rab6A-GTP were less able to redistribute GalNAc-T2^{GFP} to the ER in the presence of coexpressed BicD-C (Figure 7A, circles). Thus, in cells double expressing BicD-C and rab6A-GTP, GalNAc-T2^{GFP} remained in a juxtanuclear position (Figure 7, B–D, arrowhead). This persisted despite expression of rab6A-GTP at levels that are normally capable of redistributing GalNAc-T2^{GFP} fully into the ER (Figure 7A, black diamonds and B–D, arrow). Cells expressing only the BicD-C fragment showed a normal intact Golgi similar to noninjected cells (Figure 7A, open squares). This suggests that the dynamitin interacting BicD-C fragment inhibits the ability of rab6-GTP to redistribute Golgi proteins to the ER, most likely through its association with dynactin.

We therefore turned our focus to a possible involvement of dynein in Golgi-to-ER transport. We overexpressed p50 (dynamitin), which is known to prevent dynein/dynactin function through dissociation of the dynactin complex, disruption of dynein binding, and cargo anchoring. Dynamitin was preexpressed for 24 h, which induced a characteristic mini-Golgi phenotype indicative of impaired dynein function (Burkhardt *et al.*, 1997; Harada *et al.*, 1998). DNA encoding rab6-GTP was then injected and cells fixed for analysis after 7 h of expression. Quantitative analysis of expression levels was used as described above to assess the effect of p50 overexpression on rab6 function. As depicted in the graph of Figure 8A, p50-expressing cells display GalNAc-T2^{GFP} in dispersed mini-Golgi (squares), whereas cells expressing high levels of rab6-GTP redistribute GalNAc-T2^{GFP} to the ER (diamonds). However, high levels of rab6-GTP failed to redistribute GalNAc-T2^{GFP} to the ER when high levels of p50 were also present (circles). This suggests that p50-induced disruption of dynein function blocks rab6-induced Golgi-to-ER transport of GalNAc-T2^{GFP}. These results are represented in the micrographs of Figure 8, B–D. p50-overexpressing cells (drawing pin) showed a typical scattered Golgi phenotype indicative of dynein disruption. In cells expressing rab6A-GTP only (arrow), GalNAc-T2^{GFP} was as expected, found in the ER. However, double-expressing cells with high levels of rab6A-GTP and p50 (arrowhead) showed GalNAc-T2^{GFP} retained in scattered Golgi stacks. Some perinuclear staining (labeled in Figure 8D as NEnv) also was seen, indicating that overexpression of dynamitin does not completely block the ability of rab6A-GTP to redistribute Golgi proteins into the ER. We conclude from these observations that the dynactin complex plays a major role in Golgi-to-ER recycling through rab6. It is noted that under these conditions in the dynamitin or the BicD-C–overexpressing cells, the organization of the microtubules was normal as judged by staining with α-tubulin antibody (our unpublished data). The above-mentioned experiments show that the rab6-interacting partners BicD and dynactin are required for Golgi-to-ER transport. Given that BicD and dynactin are both involved in the recruitment of dynein, these data implicate the minus end-directed dynein motor (or a yet to be identified dynactin-associated motor) as responsible for driving rab6 retrograde transport.

DISCUSSION

We have investigated the role of the small GTP binding proteins rab6A and A' and the binding partners BicD, dy-
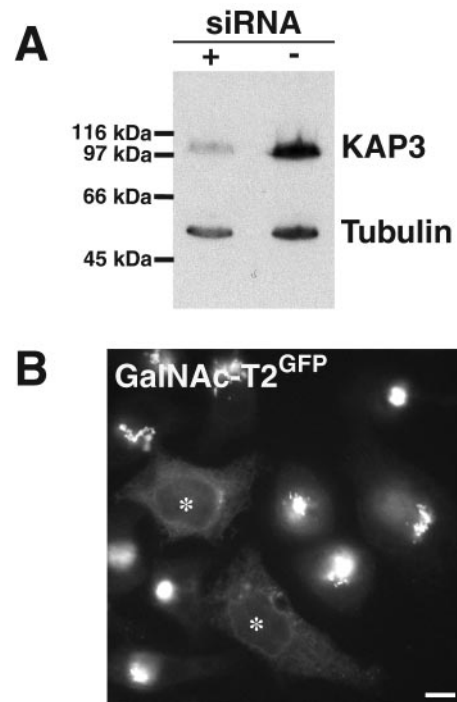

Figure 6. KIF3 is not required for rab6-induced Golgi-to-ER transport. (A) HeLa cells were treated with KAP3 siRNA or control duplexes for 48 h and then lysed in sample buffer. Western Blot analysis was performed with antibodies to KAP3 and α-tubulin for normalization of protein levels. KAP3 RNAi interference specifically decreases KAP3. (B) KAP3-depleted cells show a typical redistribution of GalNAcT2 ^{GFP} to the ER, 7 h after injection of DNA encoding rab6-GTP (asterisks).

nein/dynactin complex, and heterotrimeric kinesin KIF3 complex in Golgi-to-ER transport. We show that coincidental with the redistribution of Golgi membrane proteins to the ER, expression of rab6-GTP also redistributes endosomal proteins in proximity to the TGN to the cell periphery. The noticeably different kinetics of *trans*-, *medial*-, and *cis*-Golgi cisternae redistribution during rab6 expression suggests that rab6 preferentially transports *trans*-Golgi cisternae proteins to the ER by using a direct pathway(s) that by-passes the Golgi stack. The rab6 facilitation of Golgi-to-ER recycling requires microtubules, implicating a role of microtubule based motor proteins. We failed to find evidence for any difference between rab6A and A' by using overexpression of a dominant mutant form (Rab6-GTP). Additionally, by using RNAi, depletion of rab6A and A' together but not of the individual isoforms, resulted in a collapse of the Golgi into a compact juxtanuclear structure. Because only rab6A but not A' binds rabkinesin6, we tested for the involvement of KIF3, a kinesin complex implicated in Golgi-to-ER recycling and that also binds to the dynactin complex, but failed to see any effect upon its removal by siRNA. Rather, the rab6- (A and A') and microtubule-dependent relocation seems more related to the dynein/dynactin complex. More specifically, the dynein/dynactin-rab6 binding protein BicD and the dynactin subunit dynamitin were both found to be sensitive effectors in rab6-directed Golgi-to-ER transport. Together, these findings lead us to propose a Golgi-to-ER recycling route that operates from the *trans*-Golgi directing material directly into the ER by using dynactin and possibly the minus end-directed motor dynein. In this scenario, rab6 acts
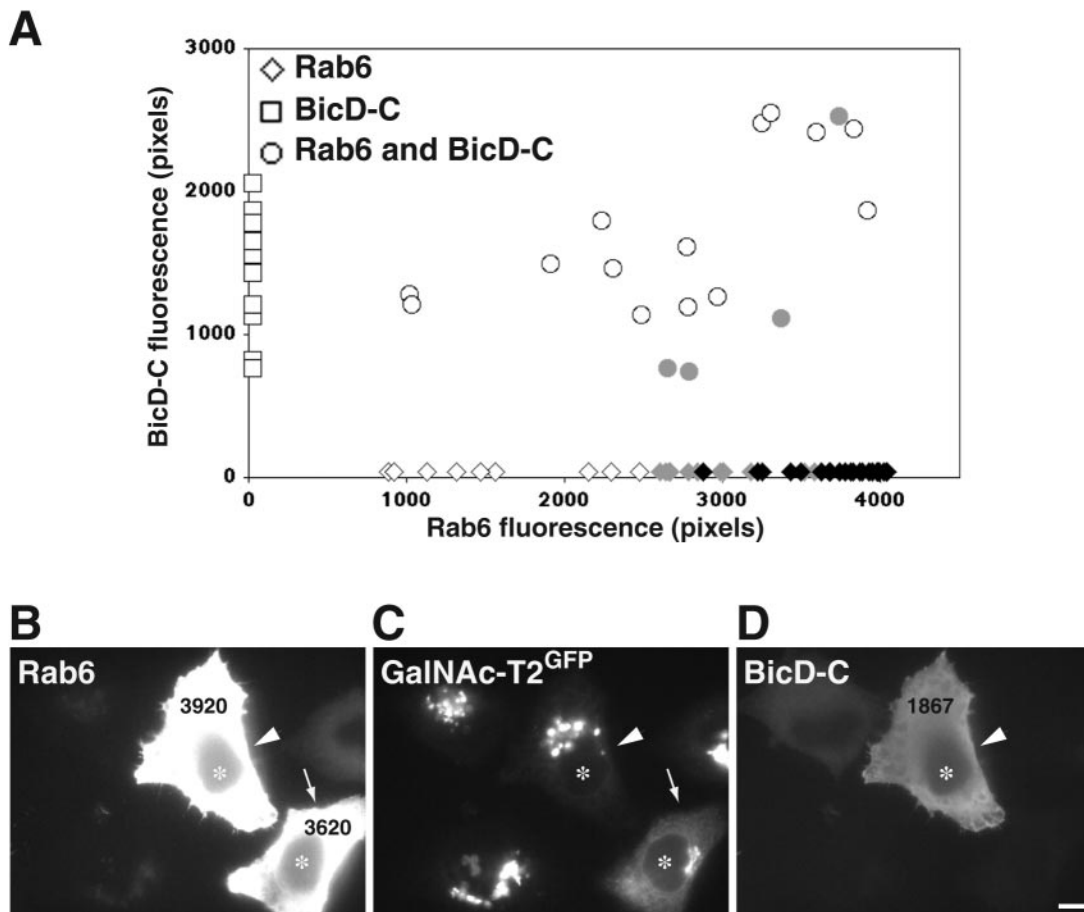
Figure 7. A rab6 and p50 binding fragment of BicD inhibits rab6A-GTP–directed Golgi-to-ER transport. (A) HeLa GalNAc-T2^{GFP} stably transfected cells were injected with an expression vector encoding mycBicD-C. After 24 h, the same cells were injected again with DNA encoding rab6A-GTP. Seven hours later, cells were fixed and stained with antibodies directed to myc-tag and rab6. Each injected cell was then scored for the level of BicD-C and rab6 protein and analyzed for the extent of Golgi-to-ER transport of GalNAc-T2^{GFP}. Rab6-GTP–expressing cells are represented by diamonds on the *x*-axis, BicD-C–expressing cells by squares on the *y*-axis, and double-injected coexpressing cells by circles. Using the same phenotypic classification of GalNAc-T2^{GFP} distribution as shown in Figure 4, an intact Golgi localization is represented by open symbols, partial GalNAc-T2^{GFP} in the ER by gray symbols, and full ER localization by black symbols. Note that exogenous expression of BicD-C alone does not affect Golgi integrity. (B–D) Representative image of HeLa GalNAc-T2^{GFP} cells (C) stained for rab6 (A) and BicD-C (D). Microinjected cells are labeled with asterisks in each panel. In the coexpressing BicD-C/rab6A-GTP cell (arrowhead), GalNAc-T2^{GFP} return to the ER is inhibited compared with the cell expressing rab6A-GTP alone, which shows the characteristic accumulation of GalNAc-T2^{GFP} in the ER (arrow). This figure is representative of three independent experiments. Bar, 10 μm.

as a facilitator of the microtubule-dependent transport step. Microtubules are not an absolute requirement for Golgi-to-ER transport, because Golgi enzymes have been proposed to recycle through the ER to form scattered Golgi ministacks in the absence of microtubules by treatment of cells with noccodazole. However, completion of Golgi recycling under these conditions is inefficient and takes many hours (Cole *et al.*, 1996).

Rab6 Regulates Recycling at a trans-Golgi/ER Interface: the "Proximity Model"

Newly synthesized proteins leave the 100 or so peripheral ER exit sites as discrete membrane packages termed vesicular tubular carriers (VTCs). These travel inwards to the central and juxtanuclear Golgi apparatus along microtubules with the help of the dynein/dynactin motor complex (Presley *et al.*, 1997; Scales *et al.*, 1997). The converse process, slow constitutive recycling from the Golgi apparatus back to the ER, does not seem to involve long-range processes, at least not any that can be easily detected. COPI vesicles that have been proposed to functionally carry Golgi material in the retrograde direction can only be observed at the ultrastructural level and usually in the near vicinity of VTCs and Golgi cisternae (Marsh *et al.*, 2001). On addition of nocodazole or during expression of rab6-GTP, the juxtanuclear Golgi apparatus seemingly melts away without any outward tracking movements (Storrie *et al.*, 1998; this study). Tubular structures labeled by GFP-rab6 or by recombinant antibodies specific to rab6-GTP have on occasion been seen emanating out from the Golgi area, and the frequency and length of such tubular structures is elevated upon rab6-GTP expression (Nizak *et al.*, 2003; White *et al.*, 1999). But evidence for a contribution of such plus end-directed processes to the recycling of intracellular Golgi material to the ER is lacking. Rather, we propose that the bulk of Golgi-to-ER recycling takes place in proximity to the Golgi apparatus. This proximity model is made possible by the fact that the ER is present throughout the cells cytoplasm, negating the
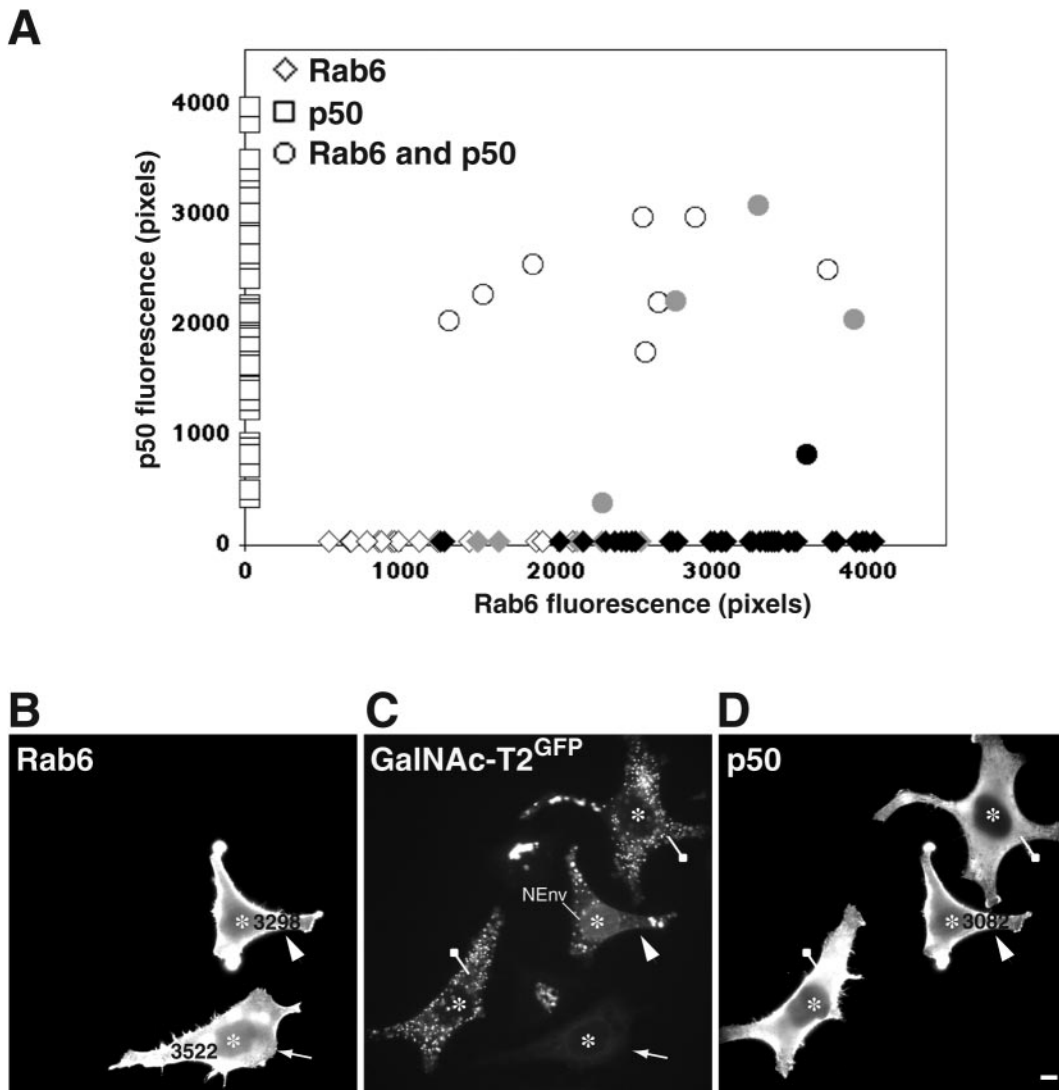
Figure 8. Disruption of the dynein/dynactin complex inhibits rab6A-GTP–mediated ER accumulation of Golgi enzymes. The experimental procedure is as described in Figure 6, except a p50-encoding expression construct was microinjected into the nucleus of HeLa GalNAc-T2^{GFP} cells. After 24 h of expression, a rab6A-GTP plasmid construct was injected into the same cells. At 7 h postinjection, cells were fixed and processed for indirect immunofluorescence with antibodies against p50 and rab6. (A) Graphical depiction of such an experiment with levels of p50 protein shown by squares on the *y*-axis, rab6 levels by diamonds on the *x*-axis, and p50/rab6A-GTP–coexpressing cells by circles. Cells were quantified for the level of rab6 and/or p50 protein and scored for the presence of GaNAc-T2^{GFP} in the juxtanuclear Golgi or in scattered mini-Golgi in the case of p50-expressing cells (open symbols), partially in the ER (gray symbols), or totally localized to the ER (black symbols). Note that p50 overexpression results in the same scattered Golgi phenotype as produced by nocodazole treatment due to inhibition of the dynein motor. (B–D) Morphological validation of the quantitative data in A. HeLa GalNAc-T2^{GFP} cells (C) stained for rab6 (A) and p50 (D). Microinjected cells are labeled with asterisks in each panel. Cells expressing only p50 show the typical Golgi fragmentation phenotype that indicates disruption of the dynein/dynactin complex (drawing pin). At high levels of coexpressed p50 and rab6A-GTP, GalNAc-T2^{GFP} remains in the scattered Golgi (arrowhead), whereas cells expressing equivalent high levels of rab6-GTP only show GaNAc-T2^{GFP} relocalized to the ER (arrow). This figure is representative of three independent experiments. Bar, 10 μm.

need for long-range movements in the retrograde direction. It is further clear that the *trans*-cisternae of the Golgi stack are interdigitated by the ER. This is based on the recent tomography studies by the groups of McIntosh and Howell (Ladinsky *et al.*, 1999) that show specialized smooth ER membrane seemingly invading the intercisternal space of the two last *trans*-cisternae of the Golgi stack. These observations confirm and extend older work by P. M. Novikoff, A. B. Novikoff, and colleagues who proposed a direct interface between the *trans*-part of the Golgi and smooth ER continuous with the rough ER based on stained thick sec-

tions (Novikoff *et al.*, 1971). This observation led to the well-known Golgi endoplasmic reticulum lysosome hypothesis postulating a direct anterograde route from the ER to outer Golgi membrane elements. Whether such a direct route exists in the anterograde direction remains to be seen. That a direct *trans*-Golgi-to-ER route exists in the retrograde direction is supported by several independent experimental observations. On addition of nocodazole, Golgi-to-ER redistribution occurs such that the *trans*-part of the Golgi stack relocates before earlier parts of the stack (Yang and Storrie, 1998). A similar *trans*-to-*cis*-sequentiality occurs also in the

presence of microtubules and overexpression of rab6-GTP (this study). The *medial-* and *cis*-cisternae may subsequently be consumed during cisternal *cis*-to-*trans* progression consistent with cisternal maturation during anterograde transport (Elsner *et al.*, 2003). In further support of this, Miles *et al.* (2001) showed that in the presence of an ER exit block three out of four Golgi glycosyltransferases/glycosidases redistribute to the ER with *trans*-first kinetics. Why not all the proteins tested in this latter study showed a *trans*-first redistribution is presently unclear. Some toxins such as Shiga and Shiga-like toxins also seem to access the ER directly from the *trans*-Golgi because ER entry is insensitive to perturbations of COPI, required for retrograde transport through the Golgi stack and from the *cis*-part of the Golgi to the ER (Girod *et al.*, 1999). Indeed, under conditions where most of the Golgi apparatus has been removed (e.g., upon addition of brefeldin-A treatment or by using the COPI-deficient Chinese hamster ovary cell-line LdlF), toxins still enter the ER, by-passing the Golgi stack (Chen *et al.*, 2002; Llorente *et al.*, 2003, Feng *et al.*, 2004). These different lines of evidence are all suggestive of a direct route from the *trans*-Golgi to the ER that is independent of the Golgi stack. Given the compelling morphological evidence for a *trans*-Golgi/ER interface, we propose that the observed effects of rab6 on recycling at the *trans*-Golgi is enabled through the proximity of the ER with the *trans*-Golgi as well as with tubular endosomes often seen in proximity to the *trans*-part of the Golgi apparatus.

The model proposed here does not exclude the possibility that rab6 also acts from earlier compartments such as the *medial-* and *cis*-cisternae. However, with rab6 being enriched in *trans*- relative to *cis*-Golgi (Goud *et al.*, 1990), such events would then contribute little to the total rab6-mediated recycling events, resulting in the *trans*-first scenario highlighted in this study.

Role of rab6 in Controlling ER Access

Among the many roles ascribed to members of the rab protein family of small GTPases is the control of SNARE-dependent membrane fusion (for review, see Zerial and McBride (2001), and more lately, the binding of motor proteins such as myosin [rab27, rab11, rab8; Langford, 2002), rabkinesin6 [rab6; Echard *et al.*, 1998], and the dynein/dynactin motor complex (rab 4, 5, 6, and 7; Bielli *et al.*, 2001; Huang *et al.*, 2001; Short *et al.*, 2002; Harrison *et al.*, 2003). Evidence for a role for rab6 in controlling membrane fusion can be found both in mammals and in yeast. The yeast orthologue Ypt6 has been implicated in endosome-to-late Golgi transport through Tlg1p, a SNARE protein found both in the late Golgi as well as on early endosomes (Siniossoglou and Pelham, 2002). In mammalian cells, the corresponding SNARE complex (Vti1a-Syntaxin16-VAMP4-Syntaxin6) is implicated in Shiga toxin transport from endosomes to the TGN. Although there exists no direct evidence that this complex interacts with rab6 in mammalian cells, rab6-GDP and -GTP mutants do affect Shiga toxin transport from endosomes to the Golgi apparatus, making this a likely scenario (Mallard *et al.*, 2002). We extended these previous studies of rab6-GTP and -GDP to include endogenous proteins MPR46, TfR, and γ-adaptin that recycle continuously in the exocytic and endocytic pathways through the Golgi. Rab6-GTP affected the steady-state distribution of these predominantly juxtanuclear proteins in addition to the early endosome compartment itself. Our data therefore support those of others, suggesting a role for rab6 in endosome-to-Golgi transport and further experiments are needed to define the directionality of the transport step regulated by rab6 in the recycling pathway. This role of rab6 may be indirect,

although, as upon overexpression of rab6-GTP, the Golgi apparatus seemingly disappears. In other words, the accumulation of MPR46, TfR, and γ-adaptin in the periphery of the cell during rab6-GTP expression may be the result of removing the acceptor compartment (*trans*-Golgi), which would then effectively prevent the exchange of material with endosomes.

In this study, we find no evidence for a differential behavior, both in the ability of the rab6 isoforms to highlight *trans*-Golgi-to-ER access as well as in affecting the redistribution of markers recycling through the endosomal and *trans*-Golgi system. The two highly homologous isoforms differ in their ability to bind rabkinesin6, such as only rab6A binds. Hence, rab6A has been suggested to mediate Golgi-to-ER recycling, whereas rab6A' would mediate endosome-to-Golgi transport. We find little, if any, evidence to support such a difference in function. In all experiments conducted, we find that rab6A-GTP and A'-GTP both affect Golgi-to-ER as well as endosome-to-Golgi transport. Careful titration of expression levels revealed no discernable differences between rab6A and A' function. Our experiments cannot reveal regulatory proteins such as an exchange factor with a specific preference for one or other of the rab6 isoforms. However, in the GTP bound active state there is clearly no discriminating function for rab6A or A'. Removal of either rab6A or A' through RNA interference also showed no marked difference on the Golgi distribution of several marker proteins, reflecting a minimal alteration of trafficking events at the Golgi. However, reduced levels of rab6A and A' together resulted in a clear effect on the Golgi distribution of GalNAc-T2^{GFP}, GM130, and TGN46. The collapsed Golgi phenotype generated by reduced levels of rab6 is similar to the reported effect of overexpression of GDP-bound forms of rab6 (Martinez *et al.*, 1994), which inhibits the recycling of Golgi enzymes through the ER (Girod *et al.*, 1999). Indeed, we also observed that decreased levels of rab6A and A' by RNAi lowered the ability of GalNAc-T2^{GFP} to return to the ER. Together with the morphological changes of the Golgi staining pattern, these results indicate a contribution by both isoforms of rab6 to the regulation of Golgi-to-ER trafficking We thus conclude that rab6A and A' exert their function in Golgi-to-ER transport in a similar manner. Rab6 is observed to bind to dynactin as well as to BicD (Matanis *et al.*, 2002; Short *et al.*, 2002), both of which are potent recruitment factors for dynein and prevented rab6 function when impaired. Overexpression of the dynamitin subunit of dynactin has been a useful tool for disrupting dynein and dynactin function. However, it is now established that dynactin also serves in the targeting of KIF3 as well as dynein, so disruption of dynamitin may interfere with KIF3-based transport events. Silencing specifically the component of the KIF3 motor complex that interacts with dynactin (KAP3) did not inhibit rab6-regulated Golgi-to-ER transport. This could suggest that the reciprocal motor of the dynein/dynactin complex working in conjunction with rab6 is a kinesin other than KIF3 or that rab6 asserts its role in retrograde transport through the minus end-directed motor dynein. This is not too far-fetched in light of the established role of BicD in inducing minus end-directed transport (Hoogenraad *et al.*, 2003), and its clear effects on rab6-GTP–induced Golgi-to-ER redistribution (this study). Other minus-end motor proteins also could be involved and further work will be needed to ascertain which dynactin-interacting motor drives rab6 and microtubule-dependent Golgi-to-ER recycling. We propose that rab6, through a dynactin-based motor complex, drives the formation of small tubular extensions that promote fusion between adjacent compartments, much like that ob-

served in the case of rab7 where small tubular extensions form in a dynein/dynactin-dependent manner, allowing phagosomes to transiently fuse with closely associated lysosomes (Harrison *et al.*, 2003).

In conclusion, we present evidence that rab6A and A' both act in Golgi-to-ER recycling and that this process is microtubule dependent and involves the motor binding protein complex dynactin. Our findings reveal a discrepancy with previous reports showing an exclusive role for rab6A but not A' in Golgi-to-ER recycling (Echard *et al.*, 2000, 2001), and future work would be needed to clarify to what extent there exists an additional role for rab6A' in endosome-to-Golgi transport and how this compares to its ability to affect Golgi-to-ER recycling. It should be noted that the ability of rab6A and A' to highlight Golgi-to-ER recycling by no means imply that these these rab proteins are strictly required for this process. In their absence and indeed, in the absence of microtubules, Golgi-to-ER recycling still occurs. As such, rab 6A and A' should be viewed as GTPases regulating Golgi-to-ER recycling.

ACKNOWLEDGMENTS

REFERENCES

Almeida, R., Levery, S. B., Mandel, U., Kresse, H., Schwientek, T., Bennett, E. P., and Clausen, H. (1999). Cloning and expression of a proteoglycan UDP-galactose:beta-xylose beta1,4-galactosyltransferase I. A seventh member of the human beta4-galactosyltransferase gene family. J. Biol. Chem. *274*, 26165–26171.

Antony, C., Cibert, C., Geraud, G., Santa Maria, A., Maro, B., Mayau, V., and Goud, B. (1992). The small GTP-binding protein rab6p is distributed from medial Golgi to the trans-Golgi network as determined by a confocal microscopic approach. J. Cell Sci. *103*, 785–796.

Bielli, A., Thornqvist, P. O., Hendrick, A. G., Finn, R., Fitzgerald, K., and McCaffrey, M. W. (2001). The small GTPase Rab4A interacts with the central region of cytoplasmic dynein light intermediate chain-1. Biochem. Biophys. Res. Commun. *281*, 1141–1153.

Burke, B., Tooze, J., and Warren, G. (1983). A monoclonal antibody which recognises each of the nuclear lamin polypeptides in mammalian cells. EMBO J. *2*, 361–367.

Burkhardt, J. K., Echeverri, C. J., Nilsson, T., and Vallee, R. B. (1997). Overexpression of the dynamitin (p50) subunit of the dynactin complex disrupts dynein-dependent maintenance of membrane organelle distribution. J. Cell Biol. *139*, 469–484.

Chen, A., Hu, T., Mikoryak, C., and Draper, R. K. (2002). Retrograde transport of protein toxins under conditions of COPI dysfunction. Biochim. Biophys. Acta *1589*, 124–139.

Cole, N. B. Sciaky, N., Marotta, A., Song, J., and Lippincott-Schwartz, J. (1996). Golgi dispersal during microtubule disruption: regeneration of Golgi stacks at peripheral endoplasmic reticulum exit sites. Mol. Biol. Cell *7*, 631–650.

Cole, N. B., Ellenberg, J., Song, J., DiEuliis, D., and Lippincott-Schwartz, J. (1998). Retrograde transport of Golgi-localized proteins to the ER. J. Cell Biol. *140*, 1–15.

Deacon, S. W., Serpinskaya, A. S., Vaughan, P. S., Lopez Fanarraga, M., Vernos, I., Vaughan, K. T., and Gelfand, V. I. (2003). Dynactin is required for bidirectional organelle transport. J. Cell Biol. *160*, 297–301.

Diao, A., Rahman, D., Pappin, D. J., Lucocq, J., and Lowe, M. (2003). The coiled-coil membrane protein golgin-84 is a novel rab effector required for Golgi ribbon formation. J. Cell Biol. *160*, 201–212.

Echard, A., el Marjou, A., and Goud, B. (2001). Expression, purification, and biochemical properties of rabkinesin-6 domains and their interactions with Rab6A. Methods Enzymol. *329*, 157–165.

Echard, A., Jollivet, F., Martinez, O., Lacapere, J. J., Rousselet, A., Janoueix-Lerosey, I., and Goud, B. (1998). Interaction of a Golgi-associated kinesin-like protein with Rab6. Science *279*, 580–585.

Echard, A., Opdam, F. J., de Leeuw, H. J., Jollivet, F., Savelkoul, P., Hendriks, W., Voorberg, J., Goud, B., and Fransen, J. A. (2000). Alternative splicing of the human Rab6A gene generates two close but functionally different isoforms. Mol. Biol. Cell *11*, 3819–3833.

Echeverri, C. J., Paschal, B. M., Vaughan, K. T., and Vallee, R. B. (1996). Molecular characterization of the 50-kD subunit of dynactin reveals function for the complex in chromosome alignment and spindle organization during mitosis. J. Cell Biol. *132*, 617–633.

Elsner, M., Hashimoto, H., and Nilsson, T. (2003). Cisternal maturation and vesicle transport: join the band wagon! Mol. Membr. Biol. *20*, 221–229.

Feng, Y., Jadhav, A. P., Rodighiero, C., Fujinaga, Y., Kirchhausen, T., and Lencer, W. I. (2004). Retrograde transport of cholera toxin from the plasma membrane to the endoplasmic reticulum requires the trans-Golgi network but not the Golgi apparatus in Exo2-treated cells. EMBO Rep. *5*, 596–601.

Fontijn, R. D., Goud, B., Echard, A., Jollivet, F., van Marle, J., Pannekoek, H., and Horrevoets, A. J. (2001). The human kinesin-like protein RB6K is under tight cell cycle control and is essential for cytokinesis. Mol. Cell. Biol. *21*, 2944–2955.

Fullekrug, J., Suganuma, T., Tang, B. L., Hong, W., Storrie, B., and Nilsson, T. (1999). Localization and recycling of gp27 (hp24gamma3): complex formation with other p24 family members. Mol. Biol. Cell. *10*, 1939–1955.

Goud, B., Zahraoui, A., Tavitian, A., and Saraste, J. (1990). Small GTP-binding protein associated with Golgi cisternae. Nature *345*, 553–556.

Girod, A., Storrie, B., Simpson, J.C., Johannes, L., Goud, B., Roberts, L. M., Lord, J. M., Nilsson, T., and Pepperkok, R. (1999). Evidence for a COP-I-independent transport route from the Golgi complex to the endoplasmic reticulum. Nat. Cell. Biol. *1*, 423–430.

Harada, A., Takei, Y., Kanai, Y., Tanaka, Y., Nonaka, S., and Hirokawa, N. (1998). Golgi vesiculation and lysosome dispersion in cells lacking cytoplasmic dynein. J. Cell Biol. *141*, 51–59.

Harrison, R. E., Bucci, C., Vieira, O.V., Schroer, T. A., and Grinstein, S. (2003). Phagosomes fuse with late endosomes and/or lysosomes by extension of membrane protrusions along microtubules: role of Rab7 and RILP. Mol. Cell. Biol. *23*, 6494–6506.

High, S., Andersen, S. S., Gorlich, D., Hartmann, E., Prehn, S., Rapoport, T. A., and Dobberstein, B. (1993). Sec61p is adjacent to nascent type I and type II signal-anchor proteins during their membrane insertion. J. Cell Biol. *121*, 743–750.

Hill, E., Clarke, M., and Barr, F.A. (2000). The Rab6-binding kinesin, Rab6-KIFL, is required for cytokinesis. EMBO J. *19*, 5711–5719.

Ho, W. C., Allan, V. J., van Meer, G., Berger, E. G., and Kreis, T. E. (1989). Reclustering of scattered Golgi elements occurs along microtubules. Eur. J. Cell Biol. *48*, 250–263.

Hoe, M. H., Slusarewicz, P., Misteli, T., Watson, R., and Warren, G. (1995). Evidence for recycling of the resident medial/trans Golgi enzyme, N-acetyl-glucosaminyltransferase I, in ldlD cells. J. Biol. Chem. *270*, 25057–25063.

Hoogenraad, C. C., Akhmanova, A., Howell, S. A., Dortland, B. R., De Zeeuw, C. I., Willemsen, R., Visser, P., Grosveld, F., and Galjart, N. (2001). Mammalian Golgi-associated Bicaudal-D2 functions in the dynein-dynactin pathway by interacting with these complexes. EMBO J. *20*, 4041–4054.

Hoogenraad, C. C., Wulf, P., Schiefermeier, N., Stepanova, T., Galjart, N., Small, J. V., Grosveld, F., de Zeeuw, C. I., and Akhmanova, A. (2003). Bicaudal D induces selective dynein-mediated microtubule minus end-directed transport. EMBO J. *22*, 6004–6015.

Huang, Z., Andrianov, V. M., Han, Y., and Howell, S. H. (2001). Identification of arabidopsis proteins that interact with the cauliflower mosaic virus (CaMV) movement protein. Plant Mol. Biol. *47*, 663–675.

Karki, S., and Holzbaur, E. L. (1995). Affinity chromatography demonstrates a direct binding between cytoplasmic dynein and the dynactin complex. J. Biol. Chem. *270*, 28806–28811.

Klumperman, J., Hille, A., Veenendaal, T., Oorschot, V., Stoorvogel, W., von Figura, K., and Geuze, H. J. (1993). Differences in the endosomal distributions of the two mannose 6-phosphate receptors. J. Cell Biol. *121*, 997–1010.

Kuge, O., Dascher, C., Orci, L., Rowe, T., Amherdt, M., Plutner, H., Ravazzola, M., Tanigawa, G., Rothman, J. E., and Balch, W. E. (1994). Sar1 promotes vesicle budding from the endoplasmic reticulum but not Golgi compartments. J. Cell Biol. *125*, 51–65.

Ladinsky, M. S., Mastronarde, D. N., McIntosh, J. R., Howell, K. E., and Staehelin, L. A. (1999). Golgi structure in three dimensions: functional insights from the normal rat kidney cell. J. Cell Biol. *144*, 1135–1149.

Langford, G. M. (2002). Myosin-V, a versatile motor for short-range vesicle transport. Traffic 3, 859–865.

Lanoix, J., Ouwendijk, J., Lin, C. C., Stark, A., Love, H. D., Ostermann, J., and Nilsson, T. (1999). GTP hydrolysis by arf-1 mediates sorting and concentration of Golgi resident enzymes into functional COP I vesicles. EMBO J. 18, 4935–4948.

Le Bot, N., Antony, C., White, J., Karsenti, E., and Vernos, I. (1998). Role of xklp3, a subunit of the *Xenopus* kinesin II heterotrimeric complex, in membrane transport between the endoplasmic reticulum and the Golgi apparatus. J. Cell Biol. 143, 1559–1573.

Lin, C. C., Love, H. D., Gushue, J. N., Bergeron, J. J., and Ostermann, J. (1999). ER/Golgi intermediates acquire Golgi enzymes by brefeldin A-sensitive retrograde transport in vitro. J. Cell Biol. 147, 1457–1472.

Llorente, A., Lauvrak, S. U., van Deurs, B., and Sandvig, K. (2003). Induction of direct endosome to endoplasmic reticulum transport in Chinese hamster ovary (CHO) cells (LdlF) with a temperature-sensitive defect in epsilon-coatomer protein (epsilon-COP). J. Biol. Chem. 278, 35850–35855.

Love, H. D., Lin, C. C., Short, C. S., and Ostermann, J. (1998). Isolation of functional Golgi-derived vesicles with a possible role in retrograde transport. J. Cell Biol. 140, 541–551.

Mallard, F., Tang, B. L., Galli, T., Tenza, D., Saint-Pol, A., Yue, X., Antony, C., Hong, W., Goud, B., and Johannes, L. (2002). Early/recycling endosomes-to-TGN transport involves two SNARE complexes and a Rab6 isoform. J. Cell Biol. 156, 653–664.

Marsh, B. J., Mastronarde, D. N., McIntosh, J. R., and Howell, K. E. (2001). Structural evidence for multiple transport mechanisms through the Golgi in the pancreatic beta-cell line, HIT-T15. Biochem. Soc. Trans. 29, 461–467.

Martinez, O., Antony, C., Pehau-Arnaudet, G., Berger, E. G., Salamero, J., and Goud, B. (1997). GTP-bound forms of rab6 induce the redistribution of Golgi proteins into the endoplasmic reticulum. Proc. Natl. Acad. Sci. USA 94, 1828–1833.

Martinez, O., Schmidt, A., Salamero, J., Hoflack, B., Roa, M., and Goud, B. (1994). The small GTP-binding protein rab6 functions in intra-Golgi transport. J. Cell Biol. 127, 1575–1588.

Matanis, T., *et al*.. (2002). Bicaudal-D regulates COPI-independent Golgi-ER transport by recruiting the dynein-dynactin motor complex. Nat. Cell. Biol. 4, 986–992.

Miles, S., McManus, H., Forsten, K. E., and Storrie, B. (2001). Evidence that the entire Golgi apparatus cycles in interphase HeLa cells: sensitivity of Golgi matrix proteins to an ER exit block. J. Cell Biol. 155 543–555.

Moremen, K. W., and Touster, O. (1985). Biosynthesis and modification of Golgi mannosidase II in HeLa and 3T3 cells. J. Biol. Chem. 260, 6654–6662.

Neef, R., Preisinger, C., Sutcliffe, J., Kopajtich, R., Nigg, E. A., Mayer, T. U., and Barr, F. A. (2003). Phosphorylation of mitotic kinesin-like protein 2 by polo-like kinase 1 is required for cytokinesis. J. Cell Biol. 162, 863–875.

Nilsson, T., Jackson, M., and Peterson, P. A. (1989). Short cytoplasmic sequences serve as retention signals for transmembrane proteins in the endoplasmic reticulum. Cell 58, 707–718.

Nizak, C., Monier, S., del Nery, E., Moutel, S., Goud, B., and Perez, F. (2003). Recombinant antibodies to the small GTPase Rab6 as conformation sensors. Science 300, 984–987.

Novikoff, P. M., Novikoff, A. B., Quintana, N., and Hauw, J. J. (1971). Golgi apparatus, GERL, and lysosomes of neurons in rat dorsal root ganglia, studied by thick section and thin section cytochemistry. J. Cell Biol. 50, 859–886.

Paschal, B. M., Holzbaur, E. L., Pfister, K. K., Clark, S., Meyer, D. I., and Vallee, R. B. (1993). Characterization of a 50-kDa polypeptide in cytoplasmic dynein preparations reveals a complex with p150GLUED and a novel actin. J. Biol. Chem. 268, 15318–15323.

Pelletier, L., Jokitalo, E., and Warren, G. (2000). The effect of Golgi depletion on exocytic transport. Nat. Cell Biol. 2, 840–846.

Presley, J. F., Cole, N. B., Schroer, T. A., Hirschberg, K., Zaal, K. J., and Lippincott-Schwartz, J. (1997). ER-to-Golgi transport visualized in living cells. Nature 389, 81–85.

Rabouille, C., Hui, N., Hunte, F., Kieckbusch, R., Berger, E. G., Warren, G., and Nilsson, T. (1995). Mapping the distribution of Golgi enzymes involved in the construction of complex oligosaccharides. J. Cell Sci. 108, 1617–1627.

Rottger, S., White, J., Wandall, H. H., Olivo, J. C., Stark, A., Bennett, E. P., Whitehouse, C., Berger, E. G., Clausen, H., and Nilsson, T. (1998). Localization of three human polypeptide GalN.Ac-transferases in HeLa cells suggests initiation of O-linked glycosylation throughout the Golgi apparatus. J. Cell Sci. 111, 45–60.

Satoh, A., Wang, Y., Malsam, J., Beard, M. B., and Warren, G. (2003). Golgin-84 is a rab1 binding partner involved in Golgi structure. Traffic 4, 153–161.

Scales, S. J., Pepperkok, R., and Kreis, T. E. (1997). Visualization of ER-to-Golgi transport in living cells reveals a sequential mode of action for COPII and COPI. Cell 90, 1137–1148.

Schiedel, A. C., Barnekow, A., and Mayer, T. (1995). Nucleotide induced conformation determines posttranslational isoprenylation of the ras related rab6 protein in insect cells. FEBS Lett. 376, 113–119.

Short, B., Preisinger, C., Schaletzky, J., Kopajtich, R., and Barr, F.A. (2002). The Rab6 GTPase regulates recruitment of the dynactin complex to Golgi membranes. Curr. Biol. 12, 1792–1795.

Siniossoglou, S., and Pelham, H. R. (2002). Vps51p links the VFT complex to the SNARE Tlg1p. J. Biol. Chem. 277, 48318–48324.

Storrie, B., Pepperkok, R., and Nilsson, T. (2000). Breaking the COPI monopoly on Golgi recycling. Trends Cell Biol. 10, 385–391.

Storrie, B., White, J., Rottger, S., Stelzer, E.H., Suganuma, T., and Nilsson, T. (1998). Recycling of Golgi-resident glycosyltransferases through the ER reveals a novel pathway and provides an explanation for nocodazole-induced Golgi scattering. J. Cell Biol. 143, 1505–1521.

Stroud, W. J., Jiang, S., Jack, G., and Storrie, B. (2003). Persistence of Golgi matrix distribution exhibits the same dependence on Sar1p activity as a Golgi glycosyltransferase. Traffic 4, 631–641.

Valsdottir, R., Hashimoto, H., Ashman, K., Koda, T., Storrie, B., and Nilsson, T. (2001). Identification of rabaptin-5, rabex-5, and GM130 as putative effectors of rab33b, a regulator of retrograde traffic between the Golgi apparatus and ER. FEBS Lett. 508, 201–209.

White, J., *et al*. (1999). Rab6 coordinates a novel Golgi to ER retrograde transport pathway in live cells. J. Cell Biol. 147, 743–760.

Yang, W., and Storrie, B. (1998). Scattered Golgi elements during microtubule disruption are initially enriched in trans-Golgi proteins. Mol. Biol. Cell 9, 191–207.

Zerial, M., and McBride, H. (2001). Rab proteins as membrane organizers. Nat. Rev. Mol. Cell. Biol. 2, 107–117.

Zheng, J. Y., Koda, T., Fujiwara, T., Kishi, M., Ikehara, Y., and Kakinuma, M. (1998). A novel Rab GTPase, Rab33B, is ubiquitously expressed and localized to the medial Golgi cisternae. J. Cell Sci. 111, 1061–1069.